THESIS FOR THE DEGREE OF DOCTOR OF PHILOSOPHY (PHD)

THE ROLE OF HYPOXIA-INDUCIBLE FACTOR ACTIVATION IN GLUCOSE-INDUCED OSTEO-/CHONDROGENIC DIFFERENTIATION OF LENS EPITHELIAL CELLS AND CHRONIC KIDNEY DISEASE-ASSOCIATED HEART VALVE CALCIFICATION

By

Haneen M. Ababneh

UNIVERSITY OF DEBRECEN

DOCTORAL SCHOOL OF MOLECULAR CELL AND IMMUNE BIOLOGY

DEBRECEN, 2024

THESIS FOR THE DEGREE OF DOCTOR OF PHILOSOPHY (PHD)

THE ROLE OF HYPOXIA-INDUCIBLE FACTOR ACTIVATION IN GLUCOSE-INDUCED OSTEO-/CHONDROGENIC DIFFERENTIATION OF LENS EPITHELIAL CELLS AND CHRONIC KIDNEY DISEASE-ASSOCIATED HEART VALVE CALCIFICATION

By

Haneen M. Ababneh

Supervisor: **Viktória Jeney DSc, PhD**

UNIVERSITY OF DEBRECEN

DOCTORAL SCHOOL OF MOLECULAR CELL AND IMMUNE BIOLOGY

DEBRECEN

2024

Table of Contents

1. Introduction

1.1. Ectopic calcification

Ectopic calcification is a pathological biomineralisation that occurs in soft tissues. Such mineralisation consists of calcium phosphate salts, including hydroxyapatite, calcium carbonates, octacalcium phosphate and calcium oxalates (1,2). Two general mechanisms of ectopic calcification are (a) metastatic calcification, a consequence of high levels of phosphate and/or calcium in the serum, and (b) dystrophic calcification, which manifests in diseased tissue because of injury or trauma under normal levels of calcium and phosphate (3).

The pathophysiology of ectopic calcification is similar to that of bone mineralisation (4). Physiological mineralisation takes place in the skeletal system, including the bone, teeth, and cartilage (5). Bone formation occurs when osteoblasts secrete an extracellular matrix mineralised by crystalline hydroxyapatite formation (6).

Ectopic calcification was thought to be a passive and degenerative process, a spontaneous precipitation of calcium phosphate salts. However, accumulated evidence in the last two decades suggests that it is a highly regulated complex mechanism driven by an imbalance between calcification inducers and inhibitors (7).

Ectopic calcification can occur in almost any soft tissue, including the brain, kidney, skin, tendons, eyes, and most importantly, the cardiovascular system (8–10) (**Fig. 1**). Among them, cardiovascular calcification is the most studied process which I will introduce in the next chapter.

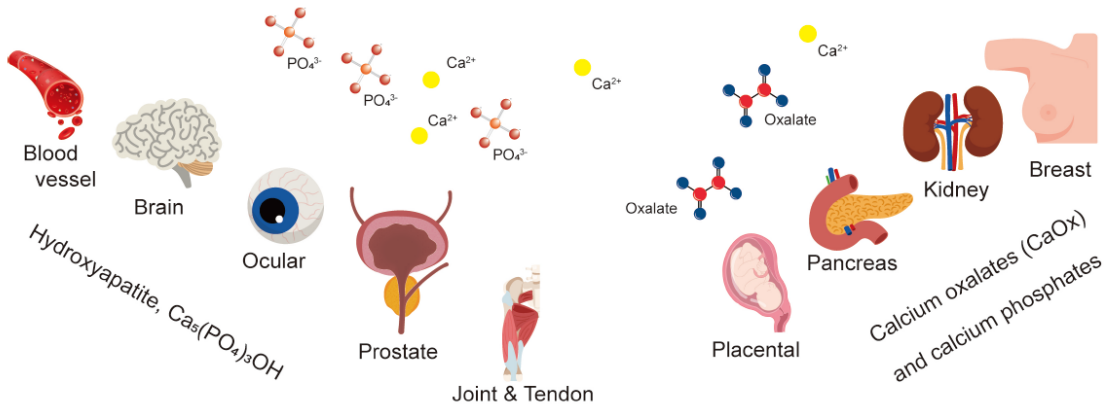

Figure 1. Ectopic calcification in soft tissues. Major sites of soft tissue calcification are shown. The primary forms of ectopic mineralisation are calcium phosphates, calcium carbonate, and calcium oxalates (243).

1.2. Cardiovascular calcification

Cardiovascular calcification is the precipitation of hydroxyapatite crystals in the walls of blood vessels, myocardium, and heart valves in the cardiovascular system which contributes to the development of cardiovascular diseases that is a leading cause of morbidity and mortality worldwide (11). Cardiovascular calcification is associated with several conditions such as hereditary disorders and aging, as well as some chronic diseases including diabetes and chronic kidney disease (CKD) (12,13).

Vascular calcification (VC) can affect different arteries, including the coronary, abdominal, iliac, and femoral arteries (14). Depending on the location of hydroxyapatite precipitation, VC is classified into intimal calcification and medial calcification (**Fig. 2**). Intimal calcification is present focally in the intimal layer and is mostly associated with atherosclerotic plaques. On the other hand, medial calcification, also known as Mönckeberg sclerosis, mainly occurs in aging, diabetes and CKD (15).

The most common heart valve disease in the Western world is calcific aortic valve disease (CAVD), which affects 25% of the senior population with no current pharmaceutical intervention (16). The disease pathogenesis is not yet completely understood, and whether it is a feature of atherosclerosis or an independent risk factor of valve calcification is still under debate (17). In advanced stages of CAVD, fibrosis and calcification of the valve can result in the obstruction of the aortic valve opening (18).

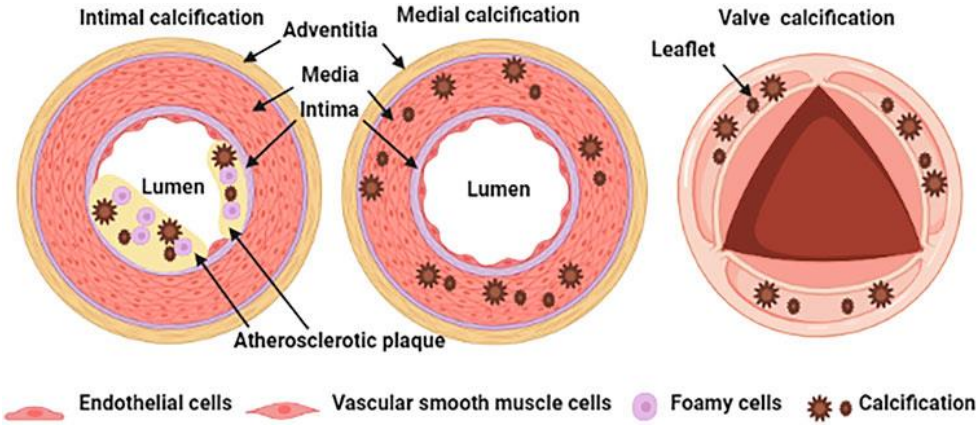

Figure 2. Types of cardiovascular calcification. Medial, intimal, and valve calcification are the most common types of cardiovascular calcification. Intimal calcification develops within an atherosclerotic plaque in the intima. Medial calcification occurs in the aortic tunica media around the smooth muscle cells. Valve calcification takes place primarily on the aortic side of heart valves (244).

Previous studies have suggested that cardiovascular calcification is an actively regulated process that involves phenotypic switching and trans-differentiation of vascular smooth muscle cells (VSMCs) and valve interstitial cells (VICs) into osteoblast-like cells. The osteo-/chondrogenic transdifferentiation of VSMCs and VICs is initiated by the upregulation of osteo-/chondrogenic transcriptional factors (19,20), including runt-related transcription factor 2 (Runx2), Sry-related HMG box-9 (Sox9), Msh homebox2 (Msx2), and bone morphogenetic proteins (BMPs). Under osteogenic conditions, VSMCs/VICs upregulate the expression of osteogenic factors such as type I collagen, alkaline phosphatase (ALP), osteopontin (OPN), and osteocalcin (OCN) (19–22).

Several calcification mechanisms have been identified. These include inflammation, apoptosis, endoplasmic reticulum (ER) stress, reactive oxygen species (ROS) production, and matrix vesicle release. Inflammation not only contributes to the progression of atherosclerosis but also triggers vascular calcification. Recent studies have shown that arterial inflammation occurs before the development of arterial calcification (23). ER stress promotes vascular calcification through apoptosis by inducing osteo-/chondrogenic transdifferentiation and autophagy (24).

1.2.1 Vascular calcification in chronic kidney disease

VC is a common complication in CKD patients. VC contributed to 3-4 fold increase in cardiovascular mortality (25). Although the exact mechanisms underlying VC in CKD are not yet completely understood, several studies have identified several risk factors contributing to VC development, such as hyperphosphatemia, uraemic toxins, hypercalcaemia, oxidative stress, inflammation, hypoxia, Klotho protein deficiency, and vitamin D supplementation (26–30).

Studies have identified a strong association between hyperphosphatemia and multiple conditions, including arteriosclerosis, vascular and valvular calcification, and a high risk of cardiovascular death, particularly in advanced CKD stages (31).

The effects of hyperphosphatemia are mediated through sodium-dependent phosphate cotransporters (Pit-1/2) which facilitates extracellular Pi entry into VSMCs (32). Accumulation of intracellular Pi promotes the expression of Runx2, OPN, and OCN. These events lead to the secretion of mineral-nucleating particles, such as matrix vesicles containing Pi and Ca as well as calcium-binding proteins and ALP. These factors induce a phenotypic switch in VSMC, leading to vascular calcification (**Fig. 3**) (33,34). Additionally, hyperphosphatemia can lead to apoptosis-

dependent VSMCs calcification through the secretion of apoptotic bodies (35,36). Some studies revealed that high Pi levels induce oxidative stress by elevating mitochondrial ROS which play a causative role in the upregulation of osteo-/chondrogenic transcription factors and markers, as well as the release of apoptotic bodies and matrix vesicles (35,37,38).

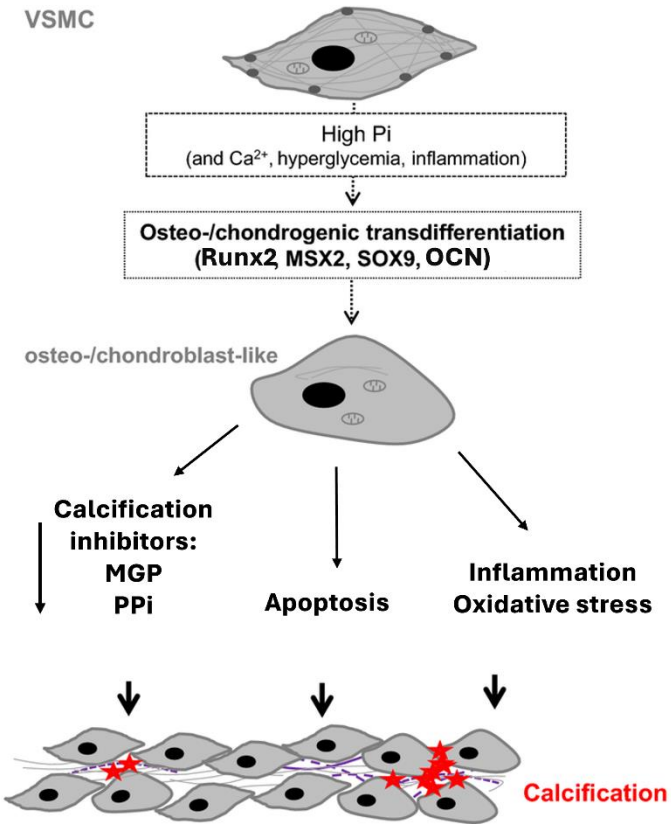

Figure 3. The mechanism of high phosphate-induced osteo-/chondrogenic transdifferentiation of VSMCs. In response to high phosphate (Pi) VSMCs can transdifferentiate into osteo-/chondroblast-like cells. This process is characterised and, at least partly, mediated by the expression of osteogenic transcription factors such as Runx2, MSX2, SOX9, and OCN. The osteoblast-like cells actively promote calcification by reduced availability of calcification inhibitors, apoptosis, inflammation and oxidative stress (33).

Additionally, passive precipitation of calcium phosphate products can be triggered by the saturation of extracellular fluids (such as urine, serum, and synovial fluids) with phosphate and calcium. Calcification inhibitors, such as Fetuin-A, pyrophosphate (PPi), OPN and Matrix Gla Proteins (MGP), prevent such passive deposition of calcium phosphate crystals (39).

1.2.2 Vascular calcification in association with type 2 diabetes (T2D)

In 2021, the International Diabetes Federation reported that the global estimate of diabetes was 537 million, with an overall prevalence of 8.3%, with the expectation that in 2045 it will reach 783 million (40). T2D is a significant independent cardiovascular risk factor and VC is one of its major complications (41,42). In fact, VC is a strong independent marker of coronary artery calcification (CAC) in T2D patients (42,43).

The molecular mechanism of T2D leading to VC has been extensively studied. Hyperglycaemia promotes osteo-/chondrogenic transdifferentiation by upregulating the expression of Runx2, BMP-2, and OCN in VSMCs (44–47). Growing evidence suggest that oxidative stress, inflammation, and, most importantly, advanced glycation end products (AGEs) play a critical role in T2D-associated VC (48–50). AGEs are a group of stable end products produced between large molecules, such as proteins, nucleic acids, lipids, and reducing sugars, under non-enzymatic reaction conditions. AGEs accumulate in the blood vessels in T2D. AGEs binds to RAGE (receptor of AGE) and activate several downstream signalling pathways involved in VC development (50–53).

Reactive oxygen species contributes to the formation of AGEs through a process known as glycoxidation. In this process, ROS react with sugars (especially glucose) to form reactive intermediates, which further interact with proteins, lipids, or nucleic acids. ROS can amplify AGEs production by promoting oxidative stress and cellular damage. Increased ROS levels in conditions like diabetes accelerate the formation of AGEs, contributing to the progression of diabetic complications (**Fig. 4**) (50,54–56).

In addition, various factors caused by T2D, such as hyperinsulinemia and diabetic nephropathy, are involved in the development of diabetic VC (57). Furthermore, diabetic patients with CKD are more susceptible to developing hyperphosphatemia (58), which is an independent risk factor for CAC development (59).

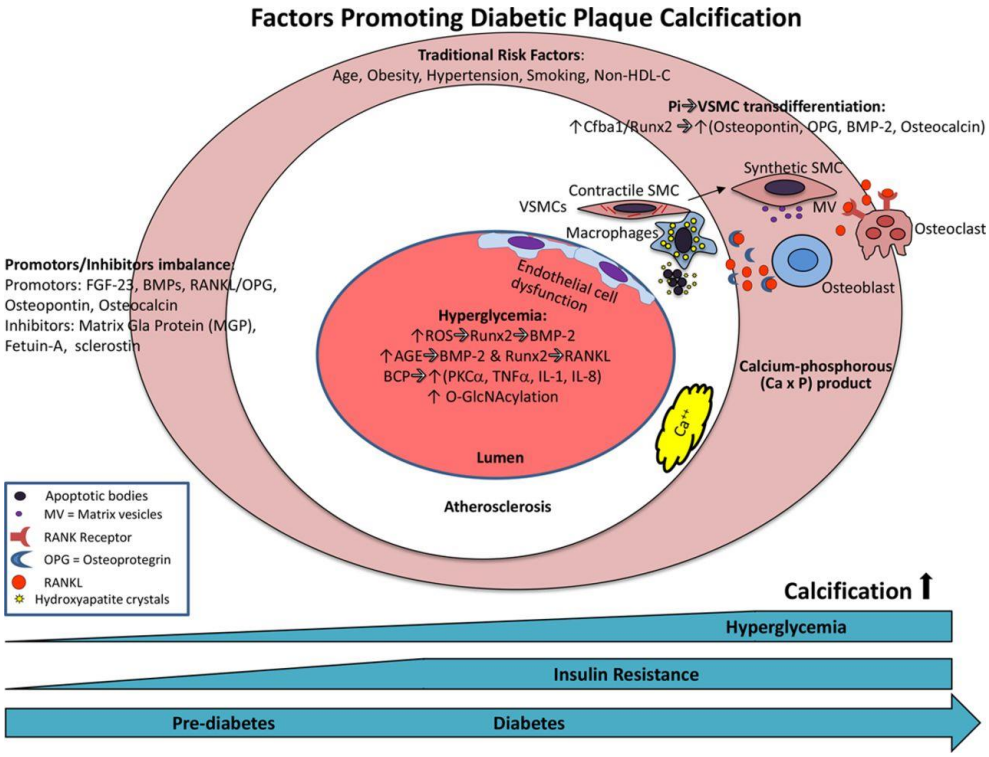

Figure 4. **Mechanisms of calcification in diabetes mellitus.** The earliest form of calcification, microcalcification, occurs in apoptotic VSMCs and macrophages in conjunction with an increase in serum calcium-phosphorous product. Increases in phosphate concentration in VSMCs induce a switch to osteoblast-like phenotype. Hyperglycaemia also affect calcification through multiple mechanisms such as oxidative stress, AGE, O-linked β-N-acetylglucosamine modification (O-GlcNAcylation), and endothelial dysfunction. EPCs; endothelial progenitor cells; FGF, fibroblast growth factor; HDL-C, high-density lipoprotein-cholesterol; IL, inter-leukin; MCCs, myeloid calcifying cells; MV, matrix vesicle; OPG, osteoprotegrin; ROS, reactive oxygen series; Runx2, Runt-related transcription factor-2; TGF, transforming growth factor; and TNF, tumor necrosis factor (42).

1.3. Calcification in the eye

The eye is a complex sensory organ responsible for vision. It detects and interprets light, converting it into electrical signals the brain processes to form visual perceptions. It consists of the cornea, conjunctiva, sclera, choroid, lens, retina, and optic nerve (60,61). Notably, pathological calcium deposition occurred across all the layers (62–66). Eye calcification is associated with various diseases, including pseudoxanthoma elasticum (PXE), chronic kidney disease, and diabetes (67–72).

1.3.1. Corneal and conjunctival calcification

Patients with CKD suffer from metastatic calcification at several sites, including the arterial valves, joints, and eyes (73). Conjunctival and corneal calcifications (CCC) are the most common forms of ectopic calcifications in the eyes of patients undergoing haemodialysis (74,75). CCC is associated with high serum calcium levels and elevated mortality risk (76). Studies have revealed a correlation between CCC and CKD, with a 26% increase in the risk of all-cause mortality (73). This indicates its significance as a potential prognostic indicator for recognising CCC development in patients undergoing maintenance haemodialysis for end-stage renal disease (ESRD) (62,73).

The association between CCC and high mortality risk needs further investigation of the underlying mechanisms causing calcification in ocular tissues. Continued investigation into the pathophysiology of CCC is promising for developing novel therapeutic strategies to improve the overall prognosis and quality of life of CKD patients undergoing haemodialysis.

Recent studies have reported that ESRD patients have a higher risk of developing calcific band keratopathy (CBK) (77). CBK is a non-specific corneal condition characterised by white-greyish opacities deposited in the superficial layers of the cornea. These opacities are typically located in the intervertebral zone (78). CBK is considered as a chronic, degenerative condition that develops slowly (79). These opacities are composed of calcium hydroxyapatite, calcium carbonate salts, and non-crystalline forms of phosphate (80). CBK can cause various systemic and ocular conditions. The most common and severe complications of CBK include high serum phosphate concentrations, elevated serum calcium levels, and secondary renal hyperparathyroidism (77,81).

1.3.3. Retinal and Bruch's membrane calcification

The deposition of calcium-containing minerals, particularly hydroxyapatite, in the retina is associated with several diseases such as age-related macular degeneration (AMD), PXE and CKD (82–85). Patients with chronic renal failure exhibited retinal arteriolar calcification (82), while PXE and AMD patients develop the calcifications in the subretinal pigment epithelial layer (83,86).

AMD, the leading cause of blindness in Europe, occur by the degeneration of the macula, and the calcification process in the subretinal pigment epithelial layer plays a critical role in its development (86–89). On the other hand, PXE is characterized by the abnormal mineralization of various tissues such as the skin, eyes, and cardiovascular system (90,91). In the eye PXE affect the

Bruch's membrane which is a thin layer of extracellular matrix situated between the choroid and the retinal pigment epithelium playing a crucial role in maintaining retinal integrity (67,92). In PXE patients, the calcification of Bruch's membrane is triggered by low levels of the calcification inhibitor PPi (93).

1.3.4. Lens calcification.

The main optical function of the lens is transmitting light, focusing it on the retina. The cornea contributes about 70% of total refraction (94), while the lens fine-tunes the focusing of light onto the retina (95,96). To facilitate light transmission the lens has one of the highest proteins concentrations of any tissue, about 60% of the lens mass is composed of proteins (97).

The lens is encased by a collagenous capsule, where epithelial cells form a monolayer on the anterior surface and the fiber cells facing posteriorly (98,99). Lens epithelial cells (LECs) start proliferating at the germinative zone. Then they migrate toward the equator, where they mature to form elongated fiber cells. Fiber cells lose most of their organelles such as mitochondria, nucleus, Golgi bodies, and both rough and smooth ER to increase light transmission (100,101).

LECs can undergo phenotype switch in response to environmental changes. For example, the epithelial-to-mesenchymal transition (EMT) is triggered by tissue damage, inflammation, or certain growth factors such as transforming growth factor beta (102,103). Studies have described that LECs are capable of undergoing osteo-, chondro-, and adipogenesis (104,105). Osteogenesis can provide an explanation for hydroxyapatite and osteocalcin presence in human cataractous lenses. The phenotypic switch of LECs into osteoblast-like cells shares similarities with physiological bone formation, and VC. Increased expression of Runx2 has been shown in LECs in response to osteogenic stimulation (**Fig. 5**) (104). Accumulating evidence suggests that phenotypic changes in LECs have a pivotal role in cataract formation.

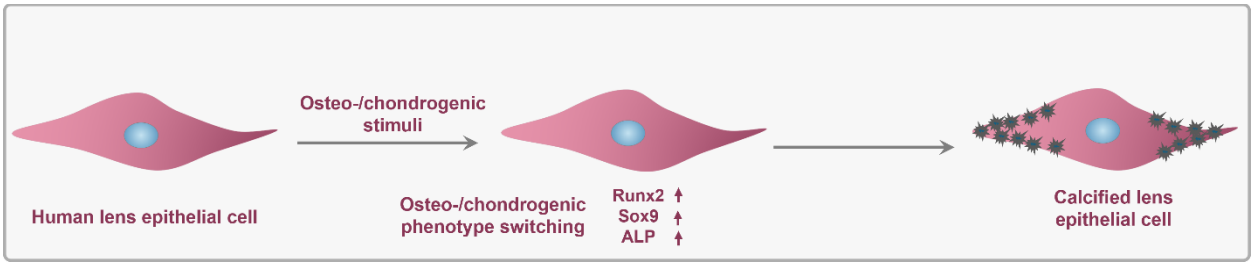

Figure 5. Schematic representation of Lens epithelial cell calcification.

Cataract is defined as lens opacification, and it is the leading cause of blindness worldwide (106,107). Several risk factors were identified for cataract formation including aging, UV, smoking, inflammation, genetics factors and diabetes (108). Among them aging is the most common risk factor for cataract formation (109), approximately 25% of the population over the age of 65 and 50% over the age of 80 are affected (110). Currently surgery is the only available treatment for cataract (111). A great deal of effort was made into determining the cause of age-related cataracts, and several relevant mechanisms have been identified.

Age-related cataract begins to manifest in the lens around the age of 50 years. This occurs due to the accumulative environmental damage to lens cells and proteins. Lens proteins are essential for maintaining its transparency; over the years, the damage accumulates slowly in these long-lived proteins. This leads to the formation of insoluble protein aggregates, which are found in cataractous lenses (112–115). On the other hand, several studies have reported that hydroxyapatite is present in cataractous lenses (115–117). As discussed previously, HuLEC can trans-differentiate into osteoblast-like cells, which can provide an explanation for the presence of hydroxyapatite in the cataractous lens.

T2D is associated with a two- to fivefold higher risk of cataract formation independent of other traditional risk factors (116). The risk of diabetic cataracts correlates with the duration of diabetes and hyperglycaemia severity, whereas glycaemic control slows the formation of cataracts (117). The pathology of cataract formation is undergoing comprehensive research, revealing various mechanisms, such as the decomposition of long-lived lens proteins, oxidative stress, and genetic defects.

1.4. Hypoxia-inducible factor 1 (HIF-1) pathway

The HIF-1 pathway has a crucial role in the cell response to hypoxia (118). HIF-1 is a heterodimeric transcription factor composed of a regulated HIFα subunit and a constantly expressed β subunit. In normoxic conditions, HIFα subunits are polyubiquitylated by the von Hipple-Lindau (VHL) and targeted for proteasomal degradation. In normoxia, this interaction between HIFα subunits and the VHL complex requires the hydroxylation of two proline residues in the oxygen dependent HIFα domain degradation (119). This reaction is catalysed by prolyl hydroxylases (PHDs) and coupled to the oxidative decarboxylation of α- ketoglutarate to succinate

and carbon dioxide. When oxygen is present PHD enzymes hydroxylate both HIF1α and HIF2α but they require α- ketoglutarate and iron (Fe^{2+}) to function (120).

In normoxic conditions, PHD2 is the primary enzyme responsible for the hydroxylation and degradation of HIFα subunit. While hypoxia prevents this reaction, which results in the dimerization of HIFα subunits with HIF-1β to form transcriptionally active complexes. HIF's transcriptional activity is regulated by factor inhibiting HIF1 (FIH1) (119,121). In normoxia FIH1

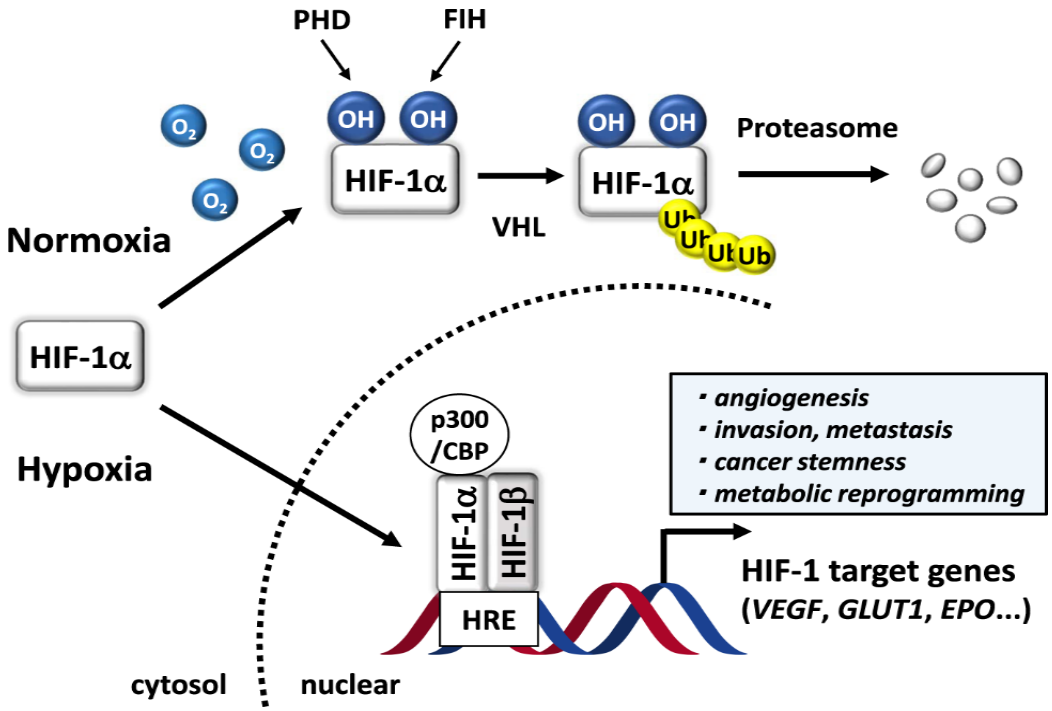

Figure 6. **HIF-1 signalling pathway.** Under normoxic conditions, HIF-1α is hydroxylated by prolyl-4- hydroxylase (PHD) and factor inhibiting HIF-1 (FIH), which interacts with von Hippel-Lindau (VHL), resulting in the degradation by the proteasome. While in hypoxic conditions, HIF-1α accumulates and translocates to the nucleus, forming a heterodimer of HIF-1α/HIF-1β. The complexes then bind to the hypoxia response element (HRE) with p300/CBP, which activates the expression of hundreds of genes, including vascular endothelial growth factor (VEGF), glucose transporter 1 (GLUT1), and erythropoietin (EPO) (245).

hydroxylates an asparagine residue within the C- C-terminal domain of HIF-1α and HIF-2α to prevent co-activators (p300 and CBP) recruitment to the C-terminal domain, reducing the transcriptional activity of HIF-1 (122). HIF pathway activation causes the transcriptional activation of various genes involved in angiogenesis, metastasis, cell survival and glycolysis, including pyruvate dehydrogenase kinase 4 (PDK4), lactate dehydrogenase A (LDHA), glucose

transporter 1 (GLUT1) and vascular endothelial growth factor A (VEGFA) (**Fig. 6**) (30,119,123–125).

1.4.1. HIF-1 pathway activation under diabetic conditions

High HIF-1α expression has been observed in diabetic patients with coronary artery calcification and in rats with VC (126). Hyperglycaemia is associated with HIF-1α stabilisation and HIF pathway activation in diverse cell types, including LECs (127). In addition, hyperglycaemia impairs the changes caused by hypoxia-induced VSMC growth (proliferation and apoptosis) through the inhibition of HIF-1α expression (128). This suggests a dynamic interplay between hyperglycaemia and hypoxia, which are two of the most critical factors of chronic complications in diabetes.

Hypoxia triggers several adaptation mechanisms, including vascular reactivity and remodelling, angiogenesis, and facilitate metabolic changes, such as enhanced glucose uptake as well as glycolysis, to promote survival in hypoxic conditions (129). Hypoxia and HIF mechanisms in patients with diabetes involve complex interactions. HIF-1α participates in VC development by regulating glucose metabolism and accelerating VSMC calcification by upregulating PDK4 expression in response to AGEs (125,130).

AGEs promote VSMCs calcification by activating the HIF-1α /PDK4 signalling pathway while impairing the metabolism of glucose (130,131). Stable HIF-1α enhances the expression of PDK4. This induces phosphorylation of SMAD1/5/8. Moreover, AGEs enhance oxidative stress in VSMCs calcification, as well as PDK4 activation which contributes to mitochondrial dysfunction and the production of excessive mitochondrial ROS (130,132,133).

The intricate interplay between ROS, oxidative stress, hypoxia, and HIF-1 in diabetes underscores the complexity of cellular responses to metabolic and environmental stressors, particularly cardiovascular and renal complications (134). Hyperglycaemia leads to ROS overproduction (135,136), whereas hypoxia triggers HIF activation, and ROS influences HIF-1α stability (137). In diabetes, the deregulation of redox-mediated HIF-1α enhances the complications induced by mitochondrial dysfunction and inflammation (**Fig. 7**) (130,138).

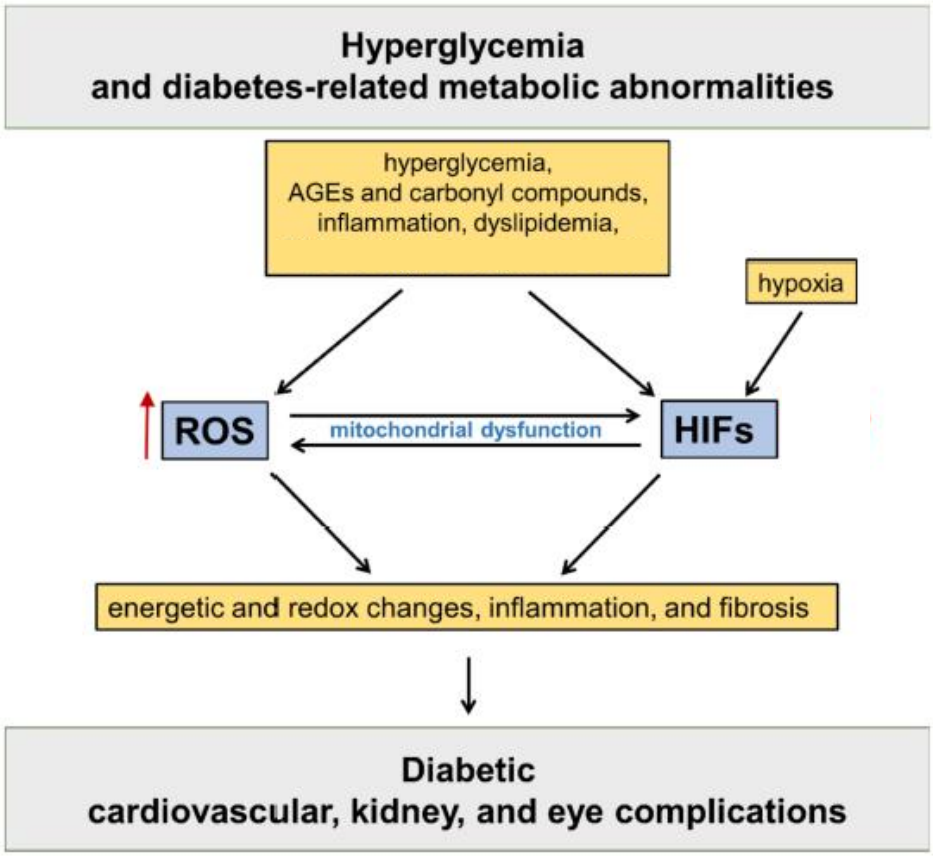

Figure 7. **Proposed mechanism of hyperglycaemia-induced complications**. Hyperglycaemia can lead to the development of cardiovascular, eye, and renal complications in which increased production of reactive oxygen species (ROS) plays a role. Both ROS and hyperglycaemia are linked to the hypoxia-inducible factor pathway (HIF). AGEs: advanced glycation end products (136).

1.4.2. Hypoxic regulation of vascular calcification

Accumulating evidence has suggested that there is a link between hypoxia and VC. For example, arterial calcification is amplified in patients with obstructive sleep apnoea, asthma, and chronic obstructive pulmonary disease (139–141).

A previous study reported increased nuclear staining for HIF-1 in aortic sections from a CKD rat model treated with a high-phosphate diet. Activation of HIF-1 was associated with increased expression of HIF-1 target genes (e.g. VEGFA and GLUT-1) and reduced VSMC marker expression. Furthermore, this study demonstrated HIF-1 activation by high phosphate levels in VSMCs, even under normoxia. Therefore, hypoxia and high phosphate levels enhance the osteo-

/chondrogenic transdifferentiation of VSMCs. HIF-1 has been identified as an early marker for CKD and a potential target against VC (142).

The role of HIF-1 pathway activation in osteo-/chondrogenic differentiation of VSMCs was also investigated in normal phosphate condition. That study revealed that hypoxia, even in the absence of elevated phosphate can induce osteo-/chondrogenic differentiation of VSMCs, in which process elevated ROS production played a critical role. ROS production occurs upstream of HIF-1 stabilisation under hypoxic conditions. ROS scavenger's attenuate hypoxia-induced calcification (30).

Additionally, researchers have reported that hypoxia-mimetic drugs such as daprodustat (DPD) activate the HIF-1 signalling pathway and increase high phosphate-induced VSMC calcification. Application of DPD at its therapeutic dose increase aorta calcification in a mice model of adenine-induced CKD (143).

2. *Hypothesis*

Hypothesis 1. We hypothesized that high glucose facilitates osteo-/chondrogenic transdifferentiation of human LECs through the activation of HIF-1 signalling.

Specific aims:

1. To establish a cellular model for studying the osteo-/chondrogenic transdifferentiation of human LECs.
2. To study the effect of high glucose level on HIF-1 activation in LECs.
3. To explore the role of HIF-1 activation in the process of osteo-/chondrogenic transdifferentiation of human LECs.
4. To provide insights into the molecular mechanism involved in the development of cataracts in diabetic individuals.

Hypothesis 2. We hypothesized that CKD triggers cardiac tissue calcification in association with increased osteogenic and hypoxia marker expressions in the heart.

Specific aims:

1. To establish a mouse model of CKD with heart tissue calcification.
2. To explore whether heart calcification is associated with increased expression of osteogenic and hypoxia markers.

3. Materials and methods

3.1. Materials

All the materials used are listed in tables 1-5.

3.2 Induction of CKD in mice

All animal experiments were performed with the University of Debrecen institutional ethics committee approval under registration number 10/2021/DEMÁB and followed Directive 2010/63/EU of the European Parliament on the protection of animals used for scientific purposes and ARRIVE guidelines. 10 male C57BL/6 mice (8–10-week-old, n=5/group) were randomly divided into two groups: control (Ctrl) and CKD. CKD was induced with a diet containing 0.2% adenine and 0.7% phosphate for six weeks, followed by 0.2% adenine and 1.8% phosphate (S8106-S075 and S8893-S006 respectively, Ssniff, Soest, Germany) for another four weeks. Mice were euthanized via CO_2 inhalation, and blood was collected for analysis by cardiac puncture.

3.3 Renal function and anaemia in mice

Plasma urea, phosphate and creatinine levels were evaluated spectrophotometrically and by a kinetic assay respectively, using a Cobas^{R} 6,000 device (Roche Diagnostics, Mannheim, Germany). Haematology parameters were assessed from citrate anti-coagulated whole blood with a Siemens Advia-2120i analyser (Siemens, Tarrytown, NY, USA) with the use of 800 Mouse C57BL6 program of Multi Species software.

3.4 Imaging and quantification of heart calcification

The mice were anesthetized with isoflurane inhalation and injected with the OsteoSense^{TM} dye in 2 nmol/ 20 g body weight dose through the retro-orbital venous sinus. Imaging was performed 24 hours post-injection. The mice were euthanized with CO_2 inhalation, then perfused with PBS, and the isolated hearts were analysed *ex-vivo* with IVIS Spectrum In Vivo Imaging System (PerkinElmer, MA, USA).

3.5 Cell culture and treatments

Human lens epithelial cells (HuLECs) were cultured in DMEM supplemented with 10% FBS, sodium pyruvate, antibiotic antimycotic solution, and L-glutamine according to the manufacturer's protocol. Cells were cultured at 37 °C in a humidified atmosphere with 5% CO_2 content. All

experiments were performed on HuLECs between passages 4 and 10. HuLECs were treated with cell culture medium with either normal glucose (NG, 1 g/L) or high glucose (HG, 4.5 g/L) content. Osteogenic stimulus (OM) was provided by supplementing the growth medium with inorganic phosphate (Pi in the form of NaH_2PO_4 and Na_2HPO_4, pH 7.4, 1.0-3.0 mmol/L as indicated) and Ca ($CaCl_2$, 0.3-0.9 mmol/L as indicated). Both the growth medium and OM were changed every other day. In some experiments, the hypoxia mimetic drugs desferrioxamine (DFO, 20 μmol/L) and $CoCl_2$ (200 μmol/L) were used.

3.6 Alizarin Red (AR) Staining and Quantification

HuLECs were washed with 200 μL of Dulbecco's Phosphate-Buffered Saline (DPBS) and then fixed with 100 μL of 4% paraformaldehyde (PFA). Then, 100 μL of Alizarin Red S solution (2%, pH 4.2) was added to the cells for 10 minutes at room temperature. Excess dye was removed by washing with distilled water several times. To quantify AR staining, 100 μL of hexadecyl-pyridinium chloride solution (100 mmol/L) was added to each well, and the optical density (OD) was measured at 560 nm.

3.9 Quantification of Ca Deposition

HuLECs were washed DPBS and decalcified with 100 μL of HCl (0.6 mol/L) for 30 minutes at room temperature. To determine the Ca content of the HCl supernatant QuantiChrome Calcium Assay Kit) was used. After the removal of the HCl supernatant, cells were lysed with 100 μL of NaOH (0.1 mol/L) and sodium dodecyl sulfate (0.1%) lysis buffer, and the protein content was measured with a BCA protein assay kit. The Ca content of the cells was normalized to the protein content and expressed as μg/mg protein.

3.10 Alkaline phosphatase activity detection

HuLECs were cultured for 7 days, and then Alkaline phosphatase detection was performed using an alkaline phosphatase detection kit, according to the manufacturer’s protocol. Briefly, samples were fixed with 4% PFA for 2 minutes, and then a ratio of 2:1:1 of Fast Red Violet solution: Naphthol phosphate solution: deionized water was added to each well for 15 minutes at room temperature. Then the cells were washed with Tris-buffered saline and 0.1% Tween (TBS-T). Images were taken with a Nikon Eclipse *Ts* 2 microscope.

3.11 Determination of Cell Viability

MTT assay was used to determine cell viability. Briefly, after cell treatment, the cells were washed with 200 μL of DPBS and 100 μL of 3-[4,5-dimethylthiazol-2-yl]-2,5- diphenyltetrazolium bromide (MTT, 0.5 mg/mL) solution was added. After 3 hours of incubation at 37 °C, the MTT solution was removed. The formazan crystals were dissolved in 100 μL of DMSO, and the optical density was measured at 570 nm.

3.12 Western Blot

To evaluate protein expression, HuLECs in 6-well plates were lysed with 240 μL of Laemmli sample buffer. Then, 30 μL of the lysate was electrophoresed in SDS-PAGE (7.5 or 10%), and blotted onto a nitrocellulose membrane. Western blotting was performed with the use of anti-Runx2 antibody, anti- ALP at a 1:500 dilution, anti-Sox9 antibody at a 1:1000 dilution, anti-HIF-1α antibody at a 1:800 dilution and anti-HIF-2α antibody at a 1:800 dilution. Then the membranes were incubated with HRP-labeled anti-rabbit or anti-mouse IgG secondary antibodies diluted 1:800 for an hour at room temperature. Next, the antigen-antibody complexes were detected by enhanced chemiluminescence using Clarity™ Western ECL Substrate. Signals were detected by X-ray film or digitally by using a C-Digit Blot Scanner. After detection, the membranes were reprobed for β-actin using anti-β-actin antibody at a dilution of 1:4000. Blots were quantified by using built-in software on the C-Digit Blot Scanner.

3.13 Immunofluorescence Staining

HuLECs were cultured on coverslips in 12-well plates. After treatment, the cells were washed with cold PBS, fixed with 4% PFA for 10 minutes, and permeabilized with 0.1% Triton X-100 solution for 15 minutes. The slides were then blocked with 1% BSA for 45 minutes, incubated with either a crystalline alpha B chain antibody (CRY AB polyclonal antibody at a dilution of 1:100) anti-Runx2 antibody, 1:200, anti-Sox9 antibody 1:150 or anti-HIF1α antibody 1:200 for 2 hours at room temperature, and then incubated with goat anti-mouse IgG-CFL antibody at a dilution of 1:300 for 1 hour at room temperature. Slides were counterstained with 4’,6-diamidino-2-phenylindole (DAPI) at a dilution of 1:1000 to stain the nucleus.

3.14 RNA silencing

Lipofectamine RNAiMAX reagent was used to transfect HuLECs with siRNA. The siRNAs for Runx2 (AM16708, ID: 115587), HIF-1α, and HIF-2α and silencer negative control #1 were purchased from Invitrogen, and silencing was performed as suggested in the manufacturer's protocol. To confirm the efficiency of silencing, we performed a Western blot analysis.

3.15 Quantification of osteocalcin

For OCN detection, HuLECs were washed with PBS, and then 100 μL of EDTA (0.5 mol/L, pH 6.9) was added to each well. OCN was determined from the EDTA-solubilized supernatant by an enzyme-linked immunosorbent assay. OCN content was normalized to protein content and expressed as ng OCN/mg protein.

3.16 Real-time qPCR

Total RNA was isolated with Tri reagent, and cDNA was obtained using a High-Capacity cDNA Reverse Transcription Kit qPCR was performed with a Bio-Rad CFX96 Real-time System using iTaq™ Universal SYBR® Green Supermix and the predesigned primers listed in Table 1. The comparative Ct method was used to calculate the expression level of the transcripts, and HPRT was used for normalization as an internal control.

3.17. Statistics

The results are presented as mean ± SD. For all in vitro studies, at least three independent experiments were carried out. GraphPad Prism software was used for statistical analysis (v.8.01, San Diego, CA, USA). The Shapiro-Wilk test was used to determine the distribution's normality. Because all of the data passed the normality and equal variance tests, parametric tests were used to calculate p values. A two-tailed Student's t-test was used to determine whether there were statistically significant differences between the two groups. One-way ANOVA was used to compare more than two groups, followed by Tukey's multiple comparisons test. We used a one-way ANOVA followed by Dunnett's post hoc test to compare each of the treatment groups to a single control group. A $p < 0.05$ value was considered significant.

Table 1

Materials			
Name	**Company**	**Catalog number**	**Concentration**
Immortalized human lens epithelial cells (HuLECs)	ATCC (Manassas, VA, USA).	T0573	
High Glucose DMEM	Sigma-Aldrich (St. Louis, MO, USA)	D6171	
Low glucose	Euro lone capricorn	ECM0749L DMEM-LPXA	
Fetal Bovine Serum	Sigma-Aldrich (St. Louis, MO, USA)	F7524	
sodium pyruvate	Sigma-Aldrich (St. Louis, MO, USA)	S8636	
L-glutamine	Sigma-Aldrich (St. Louis, MO, USA)	G7513	
Antibiotic antimycotic solution	Sigma-Aldrich (St. Louis, MO, USA)	A5955	
NaH_2PO_4	Sigma-Aldrich (St. Louis, MO, USA)	S5011	
Na_2HPO_4	Sigma-Aldrich (St. Louis, MO, USA	S5136	
$CaCl_2$	Sigma	C8106	
Daprodustat (DPD)	MedChem Express (Monmouth Junction, NJ, USA)	HY-17608	1-100 µmol/L
DPBS	Gibco (Grand Island, NY, USA)	14190-144	
DMSO	Sigma-Aldrich (St. Louis, MO, USA)	D2438	
Paraformaldehyde	Merck	16005	
Alizarin Red S	Sigma-Aldrich (St. Louis, MO, USA)	A5533	2%
Hexadecyl-pyridinium chloride	Sigma-Aldrich (St. Louis, MO, USA)	C9002	100 mmol/L
HCl	Sigma-Aldrich (St. Louis, MO, USA)	30721	0.6 mol/L
NaOH	Sigma-Aldrich (St. Louis, MO, USA)	S8045	0.1 mol/L
Sodium Dodecyl Sulfate	Sigma-Aldrich (St. Louis, MO, USA)	11667289001	0.1%
EDTA	Sigma-Aldrich (St. Louis, MO, USA)	E6758	
Tri reagent	Sigma-Aldrich (St. Louis, MO, USA)	T9424	
OsteoSense 680EX	PerkinElmer (Waltham, MA, USA)	NEV10020EX	2 nmol
0.2% adenine and 0.7% phosphate diet	Ssniff (Soest, Germany)	S8106-S075	
0.2% adenine and 1.8% phosphate diet	Ssniff (Soest, Germany)	S8893-S006	
Nitrocellulose membrane	Amersham Protran, (GE Healthcare, Chicago, IL, USA)	10600002	
4', 6-diamidino-2-phenylindole (DAPI)	Thermo Fisher Scientific	62248	1:1000 1 µg/ml
Lipofectamine RNAiMAX reagent	Invitrogen, Carlsbad, CA, USA	13778-150	
desferrioxamine (DFO)	Sigma-Aldrich (St. Louis, MO, USA)	D9533	20µM/L
$CoCL_2$	Sigma-Aldrich (St. Louis, MO, USA)	60818	200µM/L
3-[4, 5-Dimethylthiazol-2-yl]-2,5-diphenyl-tetrazolium Bromide (MTT)	Sigma-Aldrich (St. Louis, MO, USA)	M2128	0.5 mg/mL in HBSS)

Table 2

Antibodies			
Name	**Company**	**Catalog number**	**Concentration**
anti-Runx2 antibody	Santa Cruz Biotechnology, Inc., Dallas, TX, USA	Sc-390715	1:500
anti-SOX9 antibody **WB, IF**	Invitrogen (Carlsbad, CA, USA)	PA5-81966	1:1000 WB 1:200 IF
anti-HiF1α antibody **WB**	GeneTex (Irvine, CA, USA)	GTX127309	1:800 1 µ/ml
anti-HiF1α antibody **IF**	Santa Cruz Biotechnology, Inc., Dallas, TX, USA	Sc-13515	1:200
anti-HiF2α antibody	Cell Signaling (Danvers, Massachusetts, USA),	#7096	1:800 3 µ/ml
Mouse anti-rabbit igG **IF**	Santa Cruz Biotechnology, Inc., Dallas, TX, USA	SC-516248	1:300 0.6 µg/ml
GOAT anti- Mouse igG-CFL **IF**	Invitrogen (Carlsbad, CA, USA)	A28175	1:300 1 µg/ml
CRY AB Polyclonal Antibody **IF**	Invitrogen (Carlsbad, CA, USA)	PA1-16950	1:100
Rabbit IgG HRP	Amersham, GE Healthcare (Chicago, IL, USA)	NA-934	1:10 000 (0.5 µg/ml)
Mouse IgG HRP	Amersham, GE Healthcare (Chicago, IL, USA)	NA-931	1:10 000 (0.5 µg/ml)
anti-β-actin	Santa Cruz Biotechnology Inc. (Dallas, TX, USA)	sc-47778	1:4000 (0.5 µg/ml)

Table 3

Kits		
Name	**Company**	**Catalog number**
Clarity Western ECL	BioRad (Hercules, CA, USA)	170-5061
QuantiChrome Calcium Assay Kit	Gentaur (Kampenhout, Belgium)	DICA-500
BCA protein assay kit	Pierce Biotechnology (Rockford, IL, USA)	23225
iTaq™ Universal SYBR® Green Supermix	Bio-Rad (Hercules, CA, USA)	1725124
OCN Enzyme-linked immunosorbent assay	DuoSet ELISA (R&D, Minneapolis, MN, USA)	DY1419-05
High Capacity cDNA Reverse Transcription kit	Applied Biosystems (Waltham, MA, USA)	4368813
Alkaline phosphatase detection kit	Sigma-Aldrich (St. Louis, MO, USA)	SCR004
Lipofectamine RNAiMAX transfection reagent	Invitrogen (Carlsbad, CA, USA)	13778-150

Table 4

RNA silencers			
Name	**Company**	**Catalog number**	**Concentration**
Silencer Select Negative Control	Invitrogen (Carlsbad, CA, USA)	4390843	10 μmol/L
siRNA for Runx2	Invitrogen (Carlsbad, CA, USA)	AM16708, ID: 115587	10 μmol/L
siRNA for HIF1	Invitrogen (Carlsbad, CA, USA)	AM16708, ID: 106498	10 μmol/L
siRNA for HIF2	Invitrogen, Carlsbad, CA, USA	AM16708, ID: 106446	10 μmol/L

Table 5

Primers			
Name	**Sequence**	**Company**	**Concentration**
HPRT FW	5'-TCCTCCTCAGACCGCTTTT-3'	Sigma-Aldrich	10 μmol/L
HPRT Rev	5'-CCTGGTTCATCATCGCTAATC-3'	Sigma-Aldrich	10 μmol/L
GLUT1 FW	5'-GGCCATCTTTTCTGTTGGGG-3'	Sigma-Aldrich	10 μmol/L
GLUT1 Rev	5'-CCAGCAGGTTCATCATCAGC-3'	Sigma-Aldrich	10 μmol/L
VEGF FW	5'-CTACCTCCACCATGCCAAGT-3'	Sigma-Aldrich	10 μmol/L
VEGF Rev	5'-GATAGACATCCATGAACTTCACCA-3'	Sigma-Aldrich	10 μmol/L
LDHA FW	5'-GATTTCCGCCCACCTTTC-3'	Sigma-Aldrich	10 μmol/L
LDHA Rev	5'-ACAAAGCTCAAGCCCAAGG-3'	Sigma-Aldrich	10 μmol/L
PDK4 FW	5'-CTGAGAATTATTGACCGCCTCT-3'	Sigma-Aldrich	10 μmol/L
PDK4 Rev	5'-CAAGCCGTAACCAAAACCAG-3'	Sigma-Aldrich	10 μmol/L
HIF-1α FW	5′-GTTGCCACTTCCCCACAATG-3'	Sigma-Aldrich	10 μmol/L
HIF-1α Rev	5′-TTCACTGTCTAGACCACCGG-3′	Sigma-Aldrich	10 μmol/L
HIF-2α FW	5′-TCGGACACATAAGCTCCTGT-3′	Sigma-Aldrich	10 μmol/L
HIF-2α Rev	5′-CCACAGCAATGAAACCCTCC-3′	Sigma-Aldrich	10 μmol/L
Runx2 FW	5'-GCATCCTATCAGTTCCCAATG-3'	Sigma-Aldrich	10 μmol/L
Runx2 Rev	5'-GAGGTGGTGGTGCATGGT-3'	Sigma-Aldrich	10 μmol/L
Sox9 FW	5'-GCTCTACTCCACCTTCACTTAC-3'	Sigma-Aldrich	10 μmol/L
Sox9 Rev	5'-TGTGTGTAGACTGGTTGTTCC-3'	Sigma-Aldrich	10 μmol/L

4. *Results*

4.1. In vitro model for human LECs (HuLECs) calcification.

First, we established a calcification model for HuLECs osteo-/chondrogenic transdifferentiation. We cultured HuLECs in control (Ctrl) or osteogenic (OM; 2.5 mmol/L Pi, 0.3 mmol/L Ca) medium up to 6 days. Calcification of the ECM started on the third day and kept increasing until day 6 in OM-treated HuLECs whereas we did not detect ECM calcification in HuLECs under Ctrl conditions (**Fig. 8A, B**). To confirm AR staining results, we measured calcium levels from HCl-solubilized ECM samples, which revealed that ECM calcium content was more than 16-fold higher in OM-treated HuLECs than the controls (**Fig. 8C**). Finally, we measured OCN levels, the bone-specific calcium-binding protein, in EDTA-solubilized ECM of HuLECs. In response to the osteogenic stimuli, OCN levels increased by 8-fold compared to Ctrl (**Fig. 8D**).

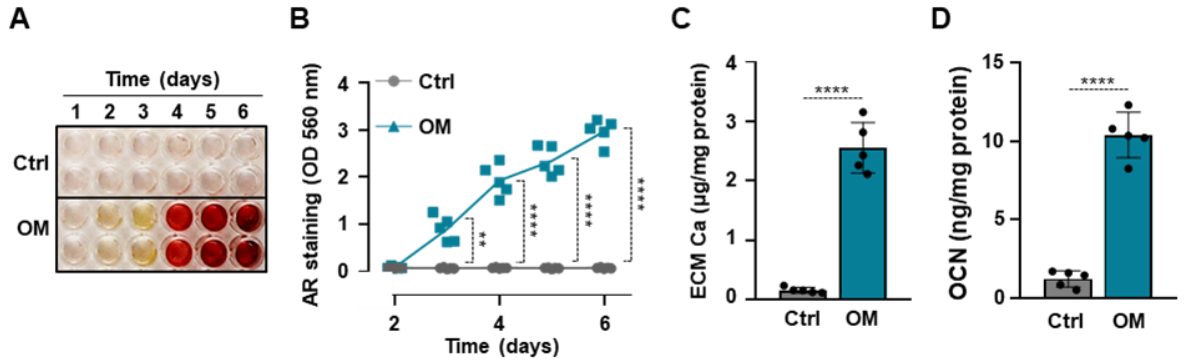

Figure 8. ***In vitro*** **HuLEC calcification model**. (A-D) Confluent HuLECs were maintained in control (Ctrl) or osteogenic conditions (OM). (A, B) Time course of Ca deposition evaluated by AR staining. (C) Ca content of the HCl-solubilized ECM. (D) OCN level in EDTA-solubilized ECM. (C, D) Data are expressed as mean ± SD, from 5 independent experiments. (B) Multiple t-tests to compare Ctrl and OM at each time point were performed to obtain *p* values. (C, D) t-test was used to obtain *p* values. ** $p < 0.01$, **** $p < 0.001$.

4.2. High glucose promotes calcification of HuLECs.

Lens epithelial cells are critical contributors to the intricate processes underlying cataractogenesis. For example, proliferation, migration, extracellular matrix accumulation, epithelial–mesenchymal transition (EMT), and osteo-/chondrogenic transdifferentiation, all of which have significant relevance to cataracts formation. In an effort to understand the impact of elevated glucose levels on the osteogenic transition of LECs, here we used HuLECs as the experimental model. HuLECs

were characterized by typical epithelial cell morphology and the expression of alpha crystalline, a major crystalline type in the human lens (**Fig. 9A-B**). Our previous research has shown the ability of HuLECs to undergo trans-differentiation into osteoblast-like cells, synthesizing an extracellular matrix rich with hydroxyapatite, a prevalent component in cataractous lenses. Confluent HuLECs were exposed to OM supplemented with excess phosphate (Pi, 1.0-3.0 mmol/L) and excess Ca (0.3-0.9 mmol/L) with normal glucose (NG, 1 g/L) and high glucose (HG, 4.5 g/L) content for seven days. Alizarin red staining revealed the onset of calcification in the HG group at lower Pi and Ca concentrations compared to the NG group, indicating that high glucose facilitated OM-induced calcification of HuLECs (**Fig. 9C**). Subsequently, the time dependency of HuLECs calcification under HG and NG conditions was explored using OM containing 2.5 mmol/L excess Pi and 0.6 mmol/L excess Ca. Alizarin red staining on days 3, 5, and 7 revealed accelerated and intensified calcification in the HG condition compared to the NG condition (**Fig. 9D**). Quantification of ECM Ca content confirmed the results of alizarin red staining, demonstrating both dose- and time-dependent HuLECs calcification and the promoting effect of HG on OM-induced calcification (**Fig. 9E-F**). Considering the association between calcification and cell death, an assessment of HuLECs viability after seven days of treatment was done. Notably, while OM induced a moderate decrease in cell viability under NG conditions, such an effect was not observed under HG conditions, implying that cell death is not implicated in the HG-induced promotion of calcification in HuLECs (**Fig. 9G**).

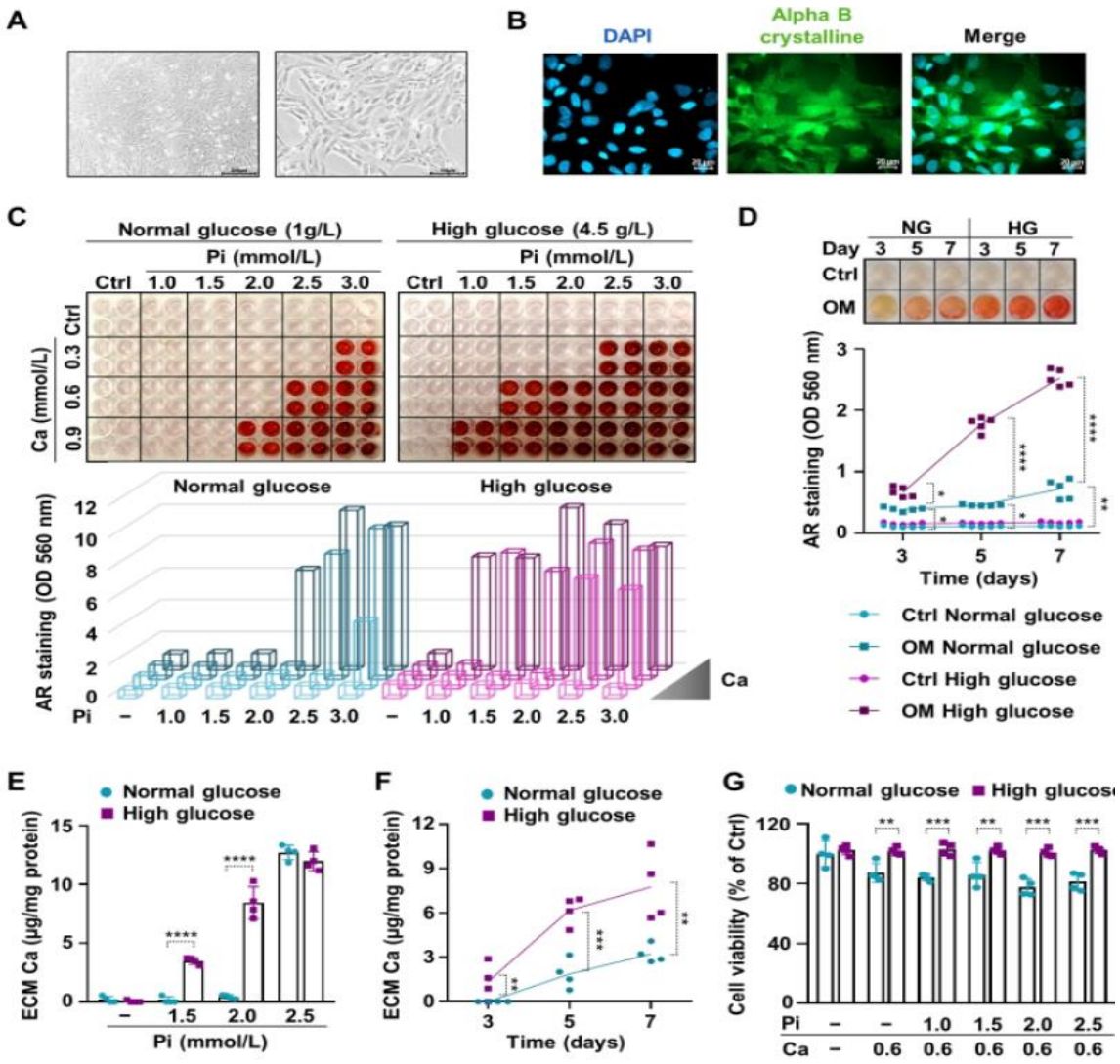

Figure 9. High glucose promotes calcification of HuLECs.

(A) Bright-field microscopy image of HuLECs (P2). (B) DAPI (4′,6-diamidino-2-phenylindole, blue) and alpha B crystalline-FITC staining (green) are shown. (C) Confluent HuLECs were cultured in control (Ctrl) or osteogenic medium (OM) containing excess phosphate (Pi, 1.0-3.0mmol/L) and excess Ca (0.3, 0.6 or 0.9 mmol/L) with normal glucose (NG, 1 g/L) and high glucose (HG, 4.5 g/L) content. Calcium deposition in the ECM (day 7) evaluated by alizarin red (AR) staining. (D) HuLECs were cultured in Ctrl or OM (2.5 mmol/L Pi and 0.6 mmol/L Ca) with NG and HG conditions. Calcium deposition in the ECM evaluated by AR staining on days 3, 5 and 7. (E) HuLECs were cultured in Ctrl or OM (Pi: 1.5-2.5 mmol/L Pi and 0.6 mmol/L Ca) with NG and HG conditions. Calcium content of the HCl-solubilized ECM (day 7). (F) HuLECs were cultured in OM (2.5 mmol/L Pi, 0.6 mmol/L Ca) with NG and HG conditions. Calcium content of the HCl-solubilized ECM measured on days 3, 5 and 7. (G) HuLECs were cultured in Ctrl or OM (1.0-2.5 mmol/L Pi, 0.6 mmol/L Ca) with NG and HG conditions. Cell viability measured by MTT assay on day 7. (C-G) Data are expressed as the mean ± SD. Three independent experiments were performed with 4-5 technical replicates. Each panel shows the result of a representative experiment. Ordinary one-way ANOVA followed by Tukey's multiple comparison test was used to calculate *p* values. **p*<0.05, ***p*<0.01, ****p*<0.005, *****p*<0.001

4.3 High glucose promotes the calcification of HuLECs in a Runx2-dependent manner.

Runx2, an important transcription factor regulating both physiological and pathological osteo-/chondrogenic transdifferentiation, thus its role in HG-induced calcification of HuLECs was investigated. OM (2.5 mmol/L Pi and 0.3 mmol/L Ca) treatment for 48 hours elicited a modest increase in Runx2 expression under normal glucose (NG) conditions (**Fig. 10A**). On the other hand, HG triggered a robust elevation in Runx2 expression under Ctrl conditions, which was further intensified in OM-treated cells (**Fig. 10A**). Then an investigation into the cellular localization of Runx2 revealed that HG induced the nuclear translocation of Runx2 (**Fig. 10B**). To investigate the involvement of Runx2 in the calcification of HuLECs, siRNA was used to downregulate Runx2 protein expression. Successful knockdown of Runx2 was confirmed by Western blot analysis (**Fig. 10C**). Diminished Runx2 expression was associated with almost a complete inhibition of OM-induced calcification under HG conditions (**Fig. 10D**), signifying the critical involvement of Runx2 in HG-induced promotion of HuLEC calcification.

Moving forward, the investigation of additional markers of osteo-/chondrogenic transdifferentiation in response to OM under NG and HG conditions revealed a moderate increase in Sox9 and ALP protein expression, as evaluated by Western blot analysis (**Fig. 11A**). Under control conditions (Ctrl), HG upregulated both Sox9 and ALP expression compared to NG Ctrl. OM stimulation under HG conditions intensified Sox9 but not ALP expression relative to HG Ctrl (**Fig. 11A**). Moreover, HG-induced the nuclear translocation of Sox9, as shown by immunofluorescence staining (**Fig. 11B**). ALP activity staining revealed that OM treatment under NG conditions increased ALP activity in HuLECs, a response further increased under HG conditions (**Fig. 11C**). The ECM concentration of OCN in HuLECs significantly increased due to OM under HG conditions, compared to that of NG conditions, as quantified by ELISA (**Fig. 11D**).

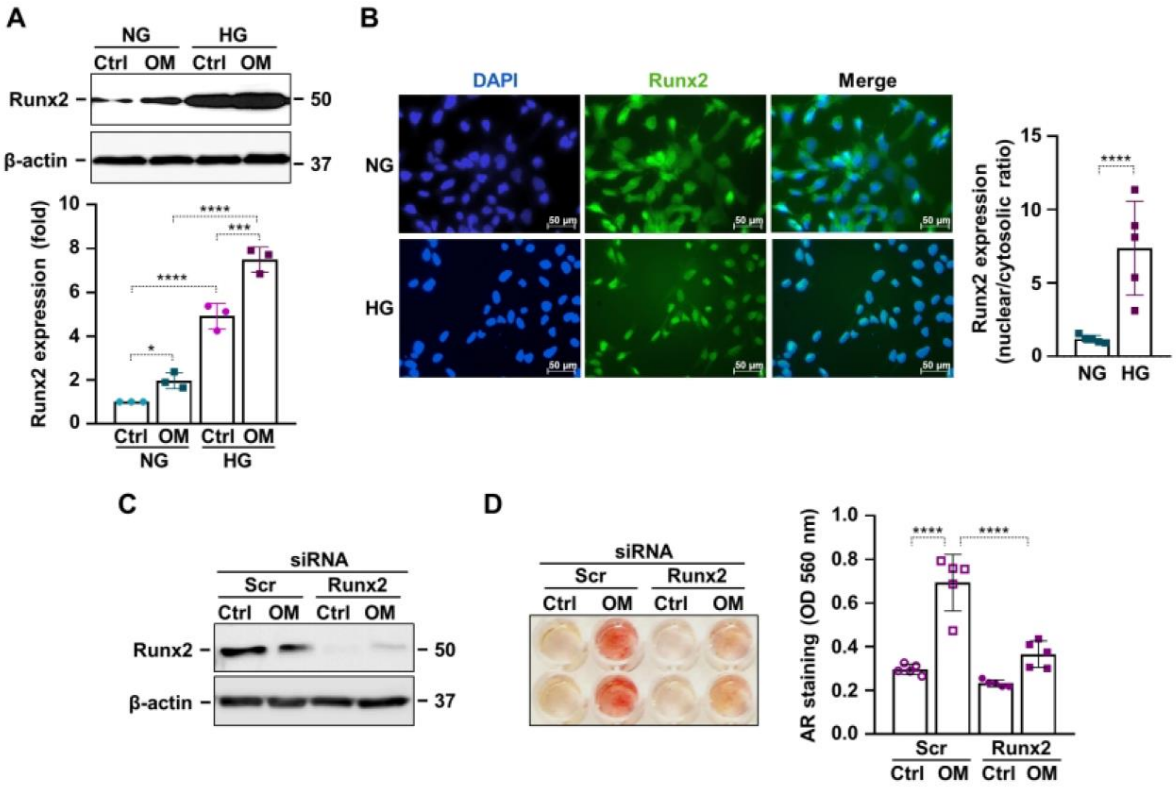

Figure 10. High glucose promotes calcification of HuLECs in a Runx2-dependent manner (A) Confluent HuLECs were kept in Ctrl or OM (2.5 mmol/l Pi, 0.3 mmol/L Ca, 48 hours) in NG and HG conditions. Protein expression of Runx2 in whole cell lysates (48 h). Membranes were reprobed for β-actin. Representative Western blots and relative expression of Runx2 normalized to β-actin from 3 independent experiments. (B) HuLECs were kept in NG and HG conditions for 24 hours. DAPI (4′,6-diamidino-2-phenylindole, blue), and Runx2-FITC staining (green) and quantification of nuclear/cytosolic Runx2 expression are shown. (C and D) HuLECs were kept in Ctrl or OM (2.5 mmol/l Pi, 0.6 mmol/L Ca) in HG conditions in the presence of Runx2 or scrambled siRNA. (C) Protein expression of Runx2 was detected by Western blot in whole cell lysates (48 h). Membranes were reprobed for β-actin. Representative Western blots and relative expression of Runx2 normalized to β-actin from 3 independent experiments. (D) Representative AR staining (day 3) and quantification of three experiments with five technical replicates. Data are expressed as the mean ± SD. Ordinary one-way ANOVA followed by Tukey's multiple comparison test was used to calculate *p* values. **p*<0.05, ****p*<0.005, *****p*<0.001

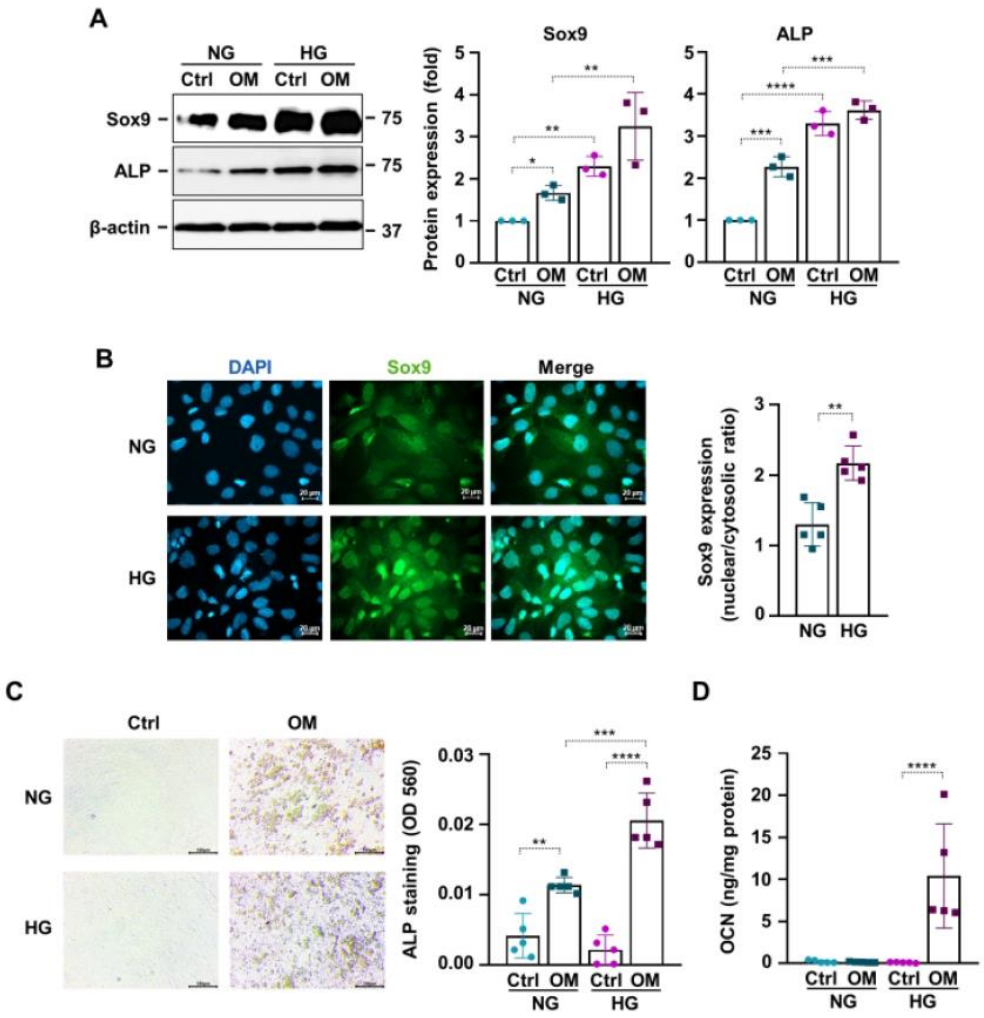

Figure 11. HG induces the expression of osteogenic markers in HuLECs

(A) Confluent HuLECs were kept in Ctrl or OM (2.5 mmol/l Pi, 0.3 mmol/L Ca) in NG and HG conditions. Protein expression of Sox9 and ALP in whole cell lysates (48 h). Membranes were reprobed for β-actin. Representative Western blots and relative expression of Sox9 and ALP normalized to β-actin from 3 independent experiments. (B) HuLECs were kept in NG and HG conditions for 24 hours. Representative DAPI (4′,6-diamidino-2-phenylindole, blue), and Sox9-FITC staining (green) and quantification of nuclear/cytosolic Sox9 expression are shown. (C) Confluent HuLECs were kept in Ctrl or OM (2.5 mmol/l Pi, 0.3 mmol/L Ca) in NG and HG conditions followed by ALP staining. Three independent experiments were performed in 5 technical replicates. Representative ALP staining (day 7) and quantification are presented. (D) Confluent HuLECs were kept in Ctrl or OM (2.5 mmol/l Pi, 0.3 mmol/L Ca) in NG and HG conditions for 10 days. OCN content of the EDTA-solubilized ECM measured by ELISA from five independent experiments. Data are expressed as the mean ± SD. Ordinary one-way ANOVA followed by Tukey's multiple comparison test was used to calculate *p* values. **p*<0.05, ***p*<0.01, ****p*<0.005, *****p*<0.001

4.4. High glucose induces HIF signalling and promotes calcification of HuLECs in a HIF-1α- and HIF-2α- dependent manner.

Previous studies showed that HG induces HIF-1α stabilization in LECs and that HIF pathway activation facilitates vascular and valve calcification (30,142), therefore here we investigated the potential involvement of HIF-1 pathway activation in the HG-induced calcification in HuLECs. To address this, HuLECs were treated with OM under NG and HG conditions. Treatment of HuLECs with HG led to a significant upregulation of both HIF-1α and HIF-2α expression under both Ctrl and OM conditions (**Fig. 12A**). Under HG conditions, OM treatment resulted in an elevated HIF-2α expression compared to the control, whereas HIF-1α expression was not further upregulated by OM (**Fig 12A**). In addition to HIF-1α stabilization, HG induced nuclear translocation of HIF-1α under OM conditions (**Fig. 12B**). Furthermore, OM treatment increased the mRNA expression of HIF-1 target genes, including Glut-1, VEGFA, LDHA and PDK4, under NG conditions which was further elevated in HG conditions (**Fig. 12C**).

To investigate the causative role of HIF-1α and HIF-2α in the calcification of HuLECs, their expression was knocked down using target-specific siRNA under HG conditions. The success of the knockdown procedure was confirmed by western blot analysis (**Fig. 12D**). After that, the OM-induced calcification of HuLECs in control (scr), and HIF-1α- and HIF-2α-deficient HuLECs revealed that knockdown of either HIF-1α or HIF-2α resulted in partial inhibition of calcification, as shown by alizarin red staining (**Fig. 12E**), which suggest that both HIF-1α and HIF-2α play vital roles in the HG-induced promotion of HuLEC calcification.

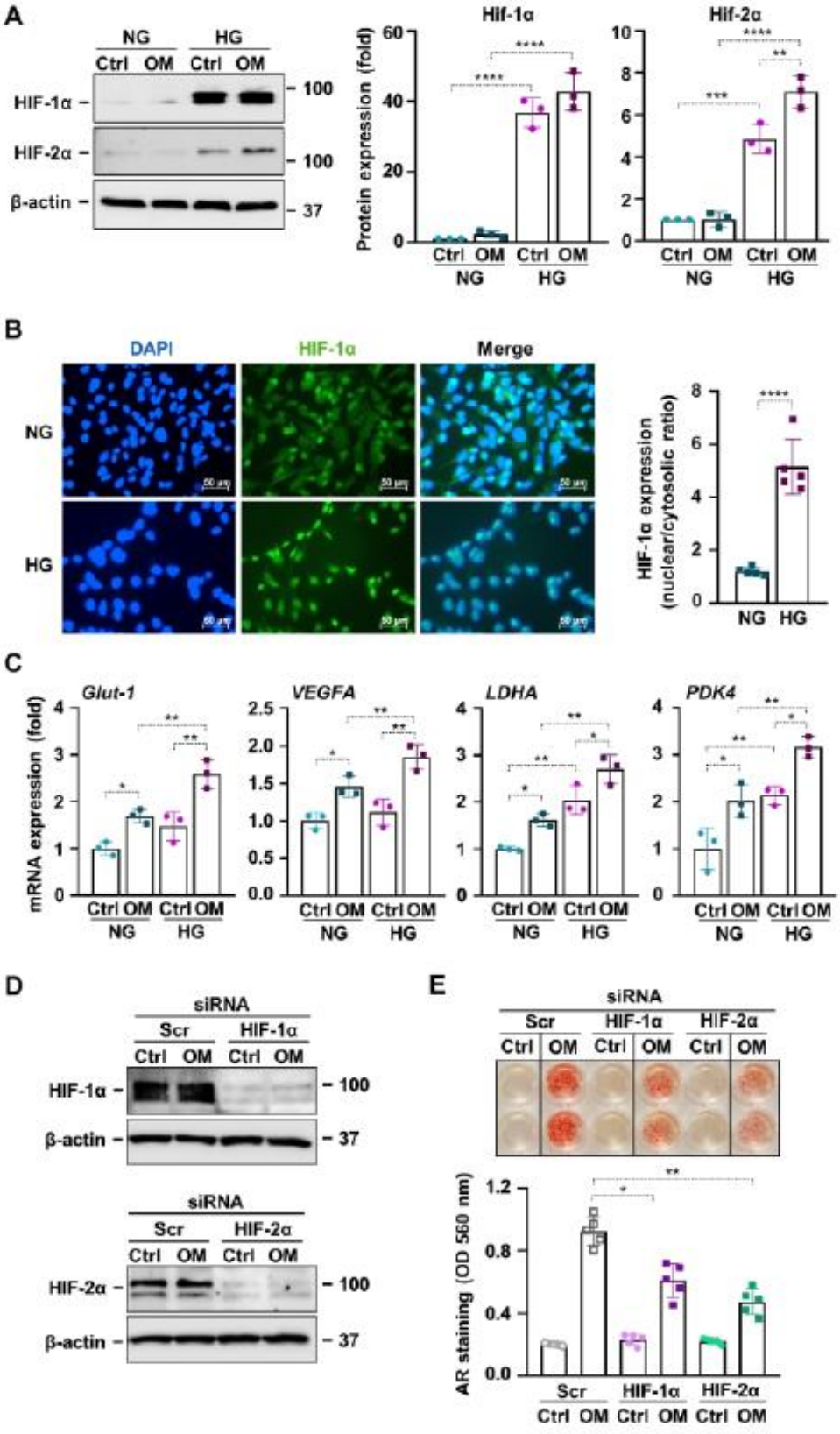
A
NG
HG
Ctrl
OM
HIF-1α
HIF-2α
β-actin
100
37
Hif-1α
Hif-2α
Protein expression (fold)
B
DAPI
HIF-1α
Merge
HIF-1α expression (nuclear/cytosolic ratio)
C
Glut-1
VEGFA
LDHA
PDK4
mRNA expression (fold)
D
siRNA
Scr
HIF-1α
HIF-2α
E
AR staining (OD 560 nm)

Figure 12. HIF-1 activation plays a key role in HG-induced calcification of HuLECs (A-B) Confluent HuLECs were kept in Ctrl or OM (2.5 mmol/l Pi, 0.3 mmol/L Ca) in NG and HG conditions. (A) Protein expression of HIF-1α and HIF-2α in whole cell lysates (48 h). Membranes were reprobed for β-actin. Representative Western blots and relative expression of HIF-1α and HIF-2α normalized to β-actin from 3 independent experiments. (B) Confluent HuLECs were exposed (24 h) to NG and HG in OM (2.5 mmol/l Pi, 0.3 mmol/L Ca). DAPI (4′,6- diamidino-2-phenylindole, blue), and HIF-1α-FITC staining (green) and quantification of nuclear/cytosolic HIF-1α expression are shown. (C) Confluent HuLECs were kept in Ctrl or OM (2.5 mmol/l Pi, 0.3 mmol/L Ca) in NG and HG conditions. Relative mRNA expression of Glut-1, VEGFA, LDHA and PDK4 (24 h). (D and E) HuLECs were kept in Ctrl or OM (2.5 mmol/l Pi, 0.6 mmol/L Ca) in HG conditions in the presence of HIF-1α, HIF-2α or scrambled siRNA. (D) Protein expression of HIF-1α and HIF-2α detected by Western blot in whole cell lysates (48 h). Membranes were reprobed for β-actin. Representative Western blots are shown from 3 independent experiments. (E) Three independent experiments were performed in 5 technical replicates. Representative AR staining (day 3) and quantification. Data are expressed as the mean ± SD. Ordinary one-way ANOVA followed by Tukey's multiple comparison test was used to calculate *p* values. **p*<0.05, ***p*<0.01, ****p*<0.005, *****p*<0.001

4.5. Hypoxia mimetics promote calcification of HuLECs.

To elucidate the involvement of HIF alpha subunit stabilization in the process of HuLECs calcification, hypoxia mimetic agents $CoCl_2$ (CC, 200 μmol/L) and desferrioxamine (DFO, 20 μmol/L) were used. Both $CoCl_2$ and DFO were able to stabilize both HIF-1α and HIF-2α under normal glucose (NG) conditions (**Fig. 13A**). An investigation into whether CC and DFO promote OM-induced HuLECs calcification under NG conditions was conducted. HuLECs were treated with Ctrl or OM in the presence or absence of CC or DFO for seven days. The results showed that both, hypoxia mimetic agents further intensified OM-induced calcification (**Fig. 13B**).

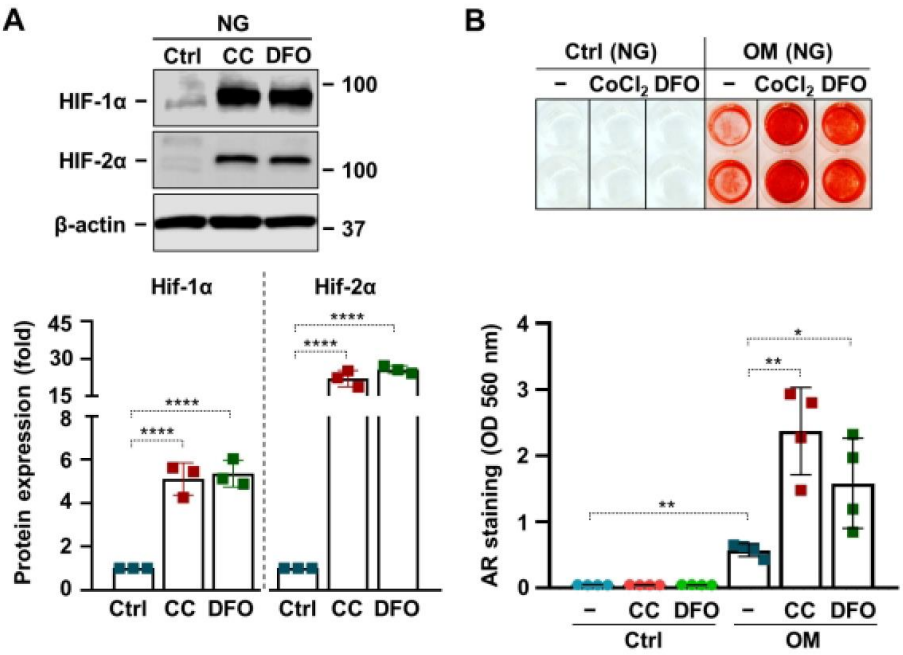

Figure 13. HIF-1 activation by hypoxia mimetic drugs enhances OM-induced calcification of HuLECs (A-B) Confluent HuLECs were treated with CoCl2 (CC, 200 μmol/L) or desferrioxamine (DFO, 20 μmol/L). (A) Protein expression of HIF-1α and HIF-2α in whole cell lysates (48 h). Membranes were reprobed for β-actin. Representative Western blots and relative expression of HIF-1α and HIF-2α normalized to β-actin from 3 independent experiments. (B) HuLECs were kept in Ctrl or OM (2.5 mmol/l Pi, 0.6 mmol/L Ca) in NG conditions in the presence of CC and DFO. Three independent experiments were performed in 4 technical replicates. Representative AR staining (day 7) and quantification. Data are expressed as the mean ± SD. Ordinary one-way ANOVA followed by Tukey's multiple comparison test was used to calculate *p* values. **p*<0.05, ***p*<0.01, *****p*<0.001

4.6. High phosphate activates osteogenic and hypoxia pathways in the hearts of CKD mice.

Cardiovascular mortality in CKD patients arises primarily from cardiac valve calcification. CKD was induced in C57BL/6 mice through a two-phase diet that involved adenine (0.2%) and moderately elevated phosphate (0.7%) for six weeks, followed by adenine (0.2%) and high phosphate (1.8%) for another four weeks. The control group (Ctrl) was fed a standard mouse diet that contained 0.3% phosphate (**Fig. 14A**). A significant reduction in body weight (**Fig. 14B**) and elevated plasma levels of urea, creatinine, and phosphate (**Fig. 14C–E**) indicated disease progression. Analysis of the mRNA levels of the osteo-/chondrogenic transcription markers Runx2 and Sox9 and hypoxia markers HIF-1α and HIF-2α in the hearts of Ctrl and CKD mice revealed that both osteogenic and hypoxia markers were substantially upregulated in the cardiac tissue of CKD mice relative to Ctrl (**Fig. 14F, G**). Moreover, OsteoSense^{TM} staining evaluation of

osteogenic activity in mice hearts revealed that the fluorescence intensity of cardiac tissue in CKD mice was significantly higher than that of Ctrl mice (4.21×10^8 vs. 6.99×10^8 p/s, $p < 0.001$, **Fig. 14H**), which indicates a higher osteogenic activity.

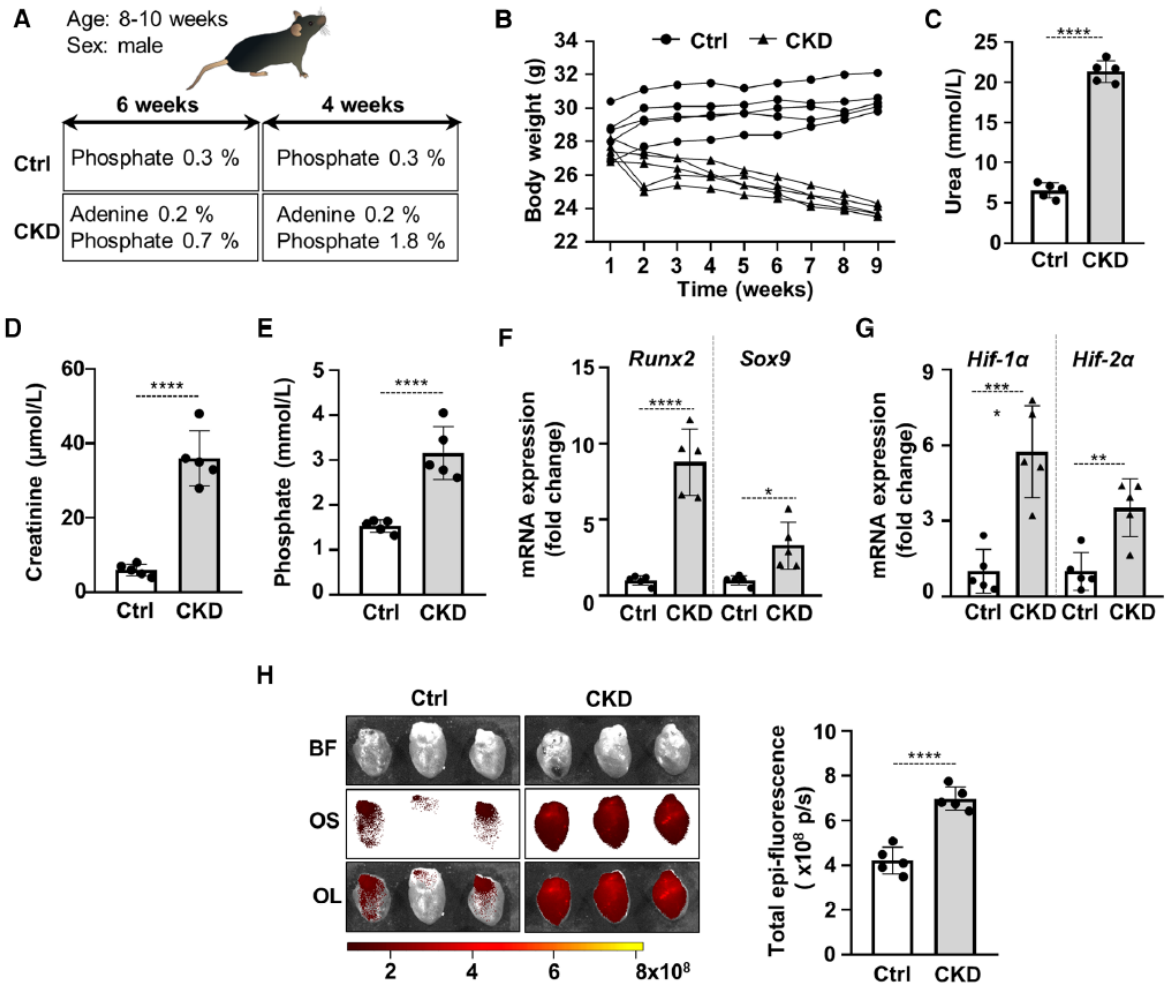

Figure 14: High phosphate activates osteogenic and hypoxia signalling in the heart of CKD mice which lead to calcification. (A) Scheme of the experimental protocol. (B) Body weight, (C) plasma urea, (D) plasma creatinine, (E) plasma phosphate levels in control (Ctrl) and CKD mice (n = 5/group). (F,G) Relative mRNA expressions of Runx2, Sox9, HIF-1α and HIF-1α normalized to HPRT from heart tissue derived from Ctrl and CKD mice (n = 5, measured in triplicates). (H) Bright-field and macroscopic fluorescence reflectance imaging of calcification and quantification in the heart of Ctrl and CKD mice (n = 5/group). Data are expressed as mean ± SD. Ordinary one-way ANOVA followed by Tukey's multiply comparison test was used to calculate *p* values. **p* < 0.05, ***p* < 0.01, ****p* < 0.005, *****p* < 0.001. BF: bright field, OS: OsteoSense, OL: overlay.

5. *Discussion*

Osteo-/chondrogenic transdifferentiation plays an essential role in physiological bone and cartilage growth, repair, and remodelling. However, pathological osteo-/chondrogenic transdifferentiation is involved in ectopic calcification, where calcium phosphate salts precipitate in the form of hydroxyapatite in the extra skeletal soft tissues. VC is the most studied form of ectopic calcification; mostly in VSMCs and VICs, thus the results of my dissertation will be discussed in comparison to these cell lines (144).

Cataracts, characterised by opacification of the lens, represent a major health issue and the leading cause of blindness globally (145,146). Diabetic patients have a higher prevalence of cataract formation at a younger age than non-diabetic individuals; moreover, epidemiological studies indicate a fivefold increased risk of cataract formation in these patients (147,148).

Several mechanisms have been attributed to the pathophysiology of diabetes-associated cataract formation, including polyol pathway upregulation, non-enzymatic glycation, and subsequent lens crystallin aggregation (145,149–151). However, recent studies suggest that other mechanisms are also involved in the pathogenesis of diabetic cataracts, such as high levels of advanced glycation end products, increased oxidative stress, and sterile inflammation (149,152–155).

Detailed analysis of the composition of senile and congenital cataracts revealed the presence of hydroxyapatite in the cataractous lenses (156–159). The current proposed mechanism for cataract formation could not explain this finding. Thus, our group investigated the possibility that HuLECs can undergo transdifferentiation into osteoblast-like cells. That work provided evidence that HuLECs upregulate the expression of osteo-/chondrogenic markers *e.g.* Runx2, Sox9, OCN, and ALP in response to osteogenic stimuli. Additionally, they found that the OCN levels and calcium content were significantly elevated in human cataractous lenses compared to control lenses, suggesting a potential role for osteo-/chondrogenic differentiation of HuLECs in lens calcification, similar to the process observed in VC (104).

VC and cataract formation are strongly associated with aging, diabetes, and CKD (71,160–162). Moreover, several studies have revealed that ectopic calcification and cataracts may share common etiological factors (163–166). Osteo-/chondrogenic transdifferentiation of VSMCs is a critical cellular event in vascular calcification. Hypercalcaemia and hyperphosphatemia are crucial

for vascular and other soft tissue calcifications in patients with CKD (167). In parallel with the clinical findings, elevated Pi and Ca levels induced osteo-/chondrogenic transdifferentiation and ECM biomineralisation of VSMCs *in vitro* (168). In agreement with these findings, here we showed that elevated Pi and Ca levels induce osteo-/chondrogenic transdifferentiation in HuLECs (**Fig. 8**).

In T2D patients, calcification of the peripheral arteries is considered an independent predictor of cardiovascular mortality, stroke, and coronary heart disease (169). ESRD patients with T2D had a higher degree of medial calcification in the inferior epigastric artery. In addition, the expression of the bone matrix proteins OPN, ALP, and type I collagen is increased in the arteries of these patients (170,171).

Hyperglycaemia promotes VC by inducing inflammation, endothelial dysfunction, and oxidative stress. In addition, it plays a critical role in developing VC (49,172–174). High glucose enhances BMP2, Runx2, OCN, and ALP expression, thereby enhancing VSMCs calcification (170). In agreement with these previous observations on VSMCs, our results show that HG is a potent inducer of calcification in HuLECs. (**Fig. 9**).

The osteo-/chondrogenic transdifferentiation of LECs may contribute to the pathogenesis of cataract formation, which is a relatively recent concept. However, thus far, this mechanism is the only explanation for the presence of hydroxyapatite in cataractous lenses (104). A recent study reported that cells within human lens capsules are capable of trilineage differentiation towards osteo-, chondro-, and adipogenesis. Additionally, they demonstrated the ability to induce osteo-/chondrogenic transdifferentiation in whole, healthy human lenses by upregulating the expression of bone-related proteins, including pigment epithelium-derived factor, collagen type I, and OCN (105).

Several calcification mechanisms have been identified, including apoptosis which plays a crucial role in the initiation of VSMC calcification (35,175,176). Apoptosis is observed in VSMC nodules before the onset of calcification (35). The presence of apoptotic bodies derived from cultured human VSMCs within these nodules indicates an association between apoptosis and calcification (35,177). Similar to matrix vesicles, these apoptotic bodies can accumulate and crystallise calcium (37,178). The inhibition of apoptosis can significantly reduce calcification, suggesting that apoptosis plays a critical role in the calcification process (35,179). Additionally, stimulating apoptosis in nodular cultures leads to a substantial increase in calcification, further

supporting the role of apoptosis in initiating vascular calcification (35). Based on this evidence, we also investigated whether apoptosis played a role in HuLEC calcification. We found that in NG conditions, osteogenic stimuli reduced HuLEC viability compared to the control. However, HG mitigated this effect; therefore, we concluded that HG-induced apoptosis does not play a role in our calcification model (**Fig. 9**).

Runx2 and Sox9 are the key transcription factors that regulate osteogenesis and chondrogenesis, respectively (180,181). Runx2, being the master transcription factor of osteogenic differentiation, regulates the expression of genes involved in osteoblast development and bone formation (182). During osteogenesis, Runx2 induces the differentiation of mesenchymal stem cells to the osteoblast lineage by promoting the expression of bone matrix genes, such as collagen type I, OPN, bone sialoprotein, and OCN (183–186). Runx2 knockout mice completely lack osteoblasts, resulting in severe skeletal abnormalities and perinatal mortality (187–190). By regulating the expression of certain genes at various stages of osteoblast differentiation, Runx2 ensures osteoblasts' proper formation and function (184). In addition, Runx2 accelerates the endochondral ossification process, in which the bone replaces cartilage during skeletal development (191,192). This is crucial for the proper formation and growth of skeletal elements. Furthermore, Runx2 has been shown to have additional biological functions besides osteoblast differentiation, including tooth development, chondrocyte maturation and tumour metastasis to the bone (191,193–195).

Sox9 is the master regulator of chondrogenesis that regulates several key events in chondrogenesis through regulating the gene expression of downstream markers in a stage-specific manner. It promotes mesenchymal cell differentiation into chondrocytes (196–198). In addition, Sox9 plays a crucial role in chondrocyte proliferation and the production of ECM components required for cartilage formation (180,199,200). Furthermore, Sox9 is involved in the differentiation of chondrocytes into pre-hypertrophic and hypertrophic states, which are essential steps in endochondral ossification, a process by which cartilage is gradually replaced by bone (201,202).

Runx2 and Sox9 also play key roles in the development of VC. The expression of these osteo-/chondrogenic transcription factors is significantly elevated in calcified human arteries compared that to in non-calcified vessels (203). In addition, several studies have revealed that VSMCs enhance Runx2 and Sox9 expression during osteo-/chondrogenic transdifferentiation (204,205).

Epithelial cells of different origins, including HuLECs express Runx2 and Sox9. High expression of Runx2 and Sox9 in these epithelial cells has been linked to a stem cell-like phenotype with regenerative potential and osteo-/chondrogenic transdifferentiation (206–210). Here, we found that HG upregulated the protein expression of both Runx2 and Sox9 and induced their nuclear translocation (**Fig. 10 and 11**). We showed that in the absence of Runx2, calcification of HuLECs is largely attenuated, which suggests that Runx2 is a key transcription factor that regulates HuLEC calcification (**Fig. 10**).

Hypoxia plays a critical role in the pathogenesis of T2D. In diabetic patients, hypoxia can affect several organs/tissues including the nerves, retina, heart, adipose tissue, blood vessels, kidney and wounds due to several factors such as increased oxygen consumption, microvascular dysfunction, and impaired oxygen delivery (211–215). This leads to the development and progression of diabetes (215). HIF-1 transcription factors are responsible for cellular responses under low-oxygen conditions through the regulation of gene expression during angiogenesis, cell survival, and glycolysis (124). T2D leads to the dysregulation of HIF-1 signalling resulting in diabetic complications including diabetic retinopathy and cardiovascular diseases. The interplay among hypoxia, HIF-1, and diabetes highlights the intricate relationship between oxygen homeostasis and metabolic dysfunction (212,214,216–218).

It has been reported that hypoxia accelerates the development of VC. HIF-1 has been identified as an early marker for CKD and a potential target against VC. Hypoxia alone induces, or in combination with high phosphate levels enhances the osteogenic trans-differentiation of VSMCs. In addition, HIF-1 activation is associated with the increased expression of HIF-1 target genes, elevation of osteo-/chondorgenic differentiation markers, and reduced VSMC marker expression. In addition, hypoxia-mimetic drugs activate the HIF-1 signalling pathway and increase high phosphate-induced VSMC calcification (30,142,143).

The lens of the eye is maintained in a hypoxic state, and HIF-1α, a subunit of HIF-1, promotes organelle degradation within the lens. However, the exact relationship between HIF-1α and cataract development is not fully understood, and there are conflicting reports on its effects (219,220).

Hyperglycaemia is associated with HIF-1α stabilisation and HIF pathway activation in diverse cell types, including (127) . Hyperglycaemia-induced HIF activation triggers upregulation of HIF-1 target genes including PDK4, LDHA, Glut-1 and VEGFA in HuLECs (127). However, in other

cell types such as dermal microvascular endothelial cells and human dermal fibroblasts HG interferes with the hypoxia-induced stabilisation of HIF-1α (218). Here we confirmed the previously reported effect of HG in stabilizing HIF-1α in HuLECs. We also showed that HG induces HIF-1α nuclear translocation and increases the expression of HIF-1α target genes (**Fig. 12**).

Previous studies have shown that high phosphate levels induced the expression of HIF-1 in the aorta of CKD rats. In addition, HIF-1 activation induced the expression of its downstream target genes and reduced VSMCs marker expression in VSMCs. In VSMCs, high phosphate alone was able to induce HIF-1 expression under normoxia; however, in combination with hypoxia, this resulted in osteo-/chondrogenic transdifferentiation of VSMCs (142). Even at normal phosphate levels, hypoxia promotes VSMCs calcification via ROS production. In addition, silencing HIF-1 activity inhibited osteo-/chondrogenic transdifferentiation of VSMCs (30). Studies have reported that HIF-1 overexpression promotes calcification of smooth muscle cells in the pulmonary artery. Additionally, clinical observations have shown that plasma HIF-1 levels significantly predict the presence of coronary artery calcification in patients with T2D (126,221). In alignment with this, our investigation revealed that when silencing either HIF-1α or HIF-2α it resulted in the inhibition of the calcification process in HuLECs. This indicates that the stabilisation of HIF-1α and HIF-2α induced by hyperglycaemia followed by HIF-1 pathway activation plays a critical role in HG-induced calcification (**Fig. 12**). Furthermore, our study demonstrates that hypoxia mimetics DFO and $CoCl_2$ accelerate high phosphate-induced calcification in HuLECs. This indicates that the calcification-promoting effect is not exclusive to glucose but depends on the activation of the HIF-1 pathway. (**Fig. 13**).

Tissue hypoxia is critical for the pathogenesis of various human diseases, including kidney disease (222,223). Due to impaired erythropoiesis, CKD is associated with anaemia and damage to the microvasculature, which contributes to the development of tissue hypoxia (224). The progression of CKD is enhanced by hypoxia, which facilitates the fibrogenesis of renal fibroblasts and promotes the epithelial-mesenchymal transition of renal tubular cells (225,226). Hypoxia is not limited to the kidneys in CKD but is also present in other tissues such as the vasculature (224,227). We were interested in whether tissue hypoxia could play a role in valve calcification, and to this end, we developed a CKD model in which valve calcification occurs.

CKD was experimentally induced in C57BL/6 mice using adenine and a high-phosphate-containing diet as previously described by Tani et al. Adenine induces CKD by damaging the interstitial layer of tubules, impairing the ability of the kidney to resorb water. This results in an increase in the urine volume and subsequent renal dysfunction. In addition, adenine diet can cause severe renal failure in mice, which is characterized by elevated blood urea nitrogen levels and irreversible kidney damage (228–231). We measured serum urea, creatinine, and phosphate levels to evaluate the kidney function of mice fed with adenine and a high-phosphate-containing diet, and found that these values were elevated, confirming that CKD induction was successful (**Fig. 14**).

To assess soft tissue calcification, we used OsteoSense™ dye, a fluorescent compound that specifically binds hydroxyapatite crystals with high affinity (232). Unlike traditional staining methods, such as Alizarin Red and von Kossa, which detect calcium or phosphate non-specifically (233–235), OsteoSense™ specifically binds hydroxyapatite crystals, providing a more accurate calcification assessment. This specificity is crucial in distinguishing hydroxyapatite from other mineral components and cellular structures, reducing the risk of false-positive results (232,236). The ability of the dye to selectively bind to hydroxyapatite crystals makes it a valuable tool for studying vascular calcification and other conditions in which hydroxyapatite deposition plays a role, offering a more targeted and efficient approach to imaging and quantifying calcification processes (232–234,236). Using this approach, we showed heart calcification in CKD mice.

Previous studies have reported that the expression of both HIF-1α and vascular endothelial growth factor is induced in stenotic valves and colocalises with angiogenesis and calcification areas. Furthermore, neovessel density was associated with the extent of valve calcification (237–240). Cardiac valve proteomic and metabolomic profile analyses have revealed that HIF-1 signalling is a key pathway in calcific aortic valve disease (241). HIF-1 activation is associated with valve calcification. For example, the non-hypoxic activation of HIF-1α has been shown to play a causative role in lipopolysaccharide- and interferon-gamma-induced calcification of VICs (242). In agreement with these previous findings, here we showed elevation of HIF-1α and HIF-2α together with increased expression of Sox9 and Runx2 in the heart derived from mice with CKD (**Fig. 14**).

In conclusion, our studies highlighted the role of HIF-1 pathway activation in soft tissue calcification which can be relevant in diabetes-induced cataract formation as well as in CKD-associated valve calcification (**Fig. 15**).

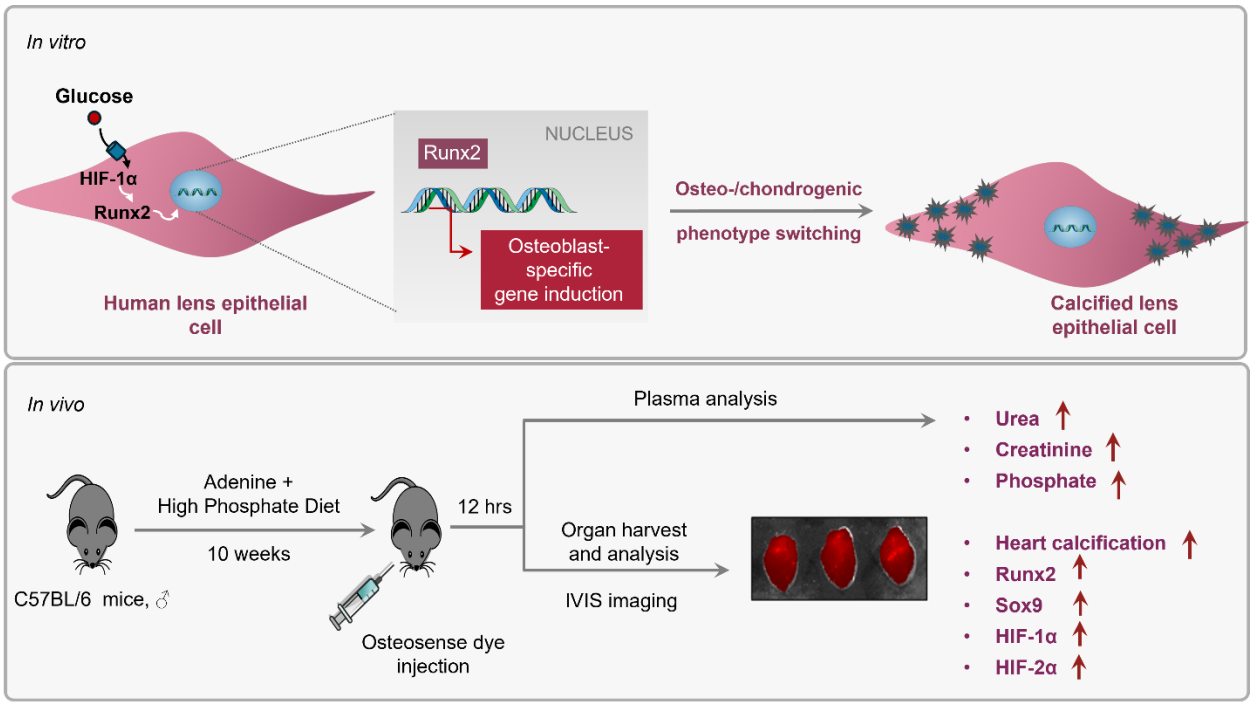

Figure 15: Graphical summary. Schematic representation for the *in vitro* and *in vivo* experimental models.

6. Summary

- Ectopic calcification, including vascular calcification, is a significant health concern associated with aging, diabetes, and chronic kidney disease (CKD).
- An association exists between osteo-/chondrogenic transdifferentiation and ectopic calcification in vascular calcification and cataract formation.
- Type 2 diabetes has been associated with an increased prevalence of cataracts, with the risk increasing with longer duration and severity of hyperglycaemia.
- Hydroxyapatite deposition in cataractous lenses results from osteo-/chondrogenic transdifferentiation and calcification of lens epithelial cells.
- This study investigated whether hyperglycaemia promotes osteo-/chondrogenic transdifferentiation of HuLECs and whether CKD triggers cardiac tissue calcification.
- High glucose levels increased the expression of osteo-/chondrogenic markers and nuclear translocation of Runx2 and Sox9 in HuLECs.
- High glucose-induced calcification was attenuated in Runx2-deficient HuLECs.
- High glucose levels stabilise hypoxia-inducible factor 1 (HIF-1) and trigger the nuclear translocation of HIF-1α, leading to increased expression of HIF-1 target genes.
- HIF-1α or HIF-2α silencing attenuates high glucose-induced calcification in HuLEC cells, whereas hypoxia mimetics DFO and $CoCl_2$ enhance calcification under normal glucose conditions.
- We established a CKD mouse model using adenine and high-phosphate-containing diet, and CKD was confirmed by elevated serum urea, creatinine, and phosphate levels.
- The CKD mouse hearts exhibited calcification, which was visualised using OsteoSense^{TM} dye, along with increased expression of hypoxia markers HIF-1α and HIF-2α and osteo-/chondrogenic markers Sox9 and Runx2.
- Our findings suggest a potential role for HIF-1 pathway activation in soft tissue calcification, which may be relevant to diabetes-induced cataract formation and CKD-associated valve calcification.

7. Keywords

- Chronic kidney disease (CKD)
- Diabetes
- Ectopic calcification
- Hyperphosphatemia
- Hypoxia
- Hypoxia inducible factor (HIF)
- Lens calcification
- Lens epithelial cells (LECs)
- Osteo-/chondrogenic transdifferentiation

8. List of abbreviations

AGEs: Advanced glycation end products

ALP: Alkaline phosphatase

AMD: Age-related macular degeneration

AR: Alizarin Red

BMP2: Bone morphogenetic protein 2

CAC: Coronary artery calcification

CAVD: Calcific aortic valve disease

CBK: Calcific band keratopathy

CC: $CoCl_2$

CCC: Conjunctival and corneal calcifications

CKD: Chronic kidney disease

Ctrl: Control

DAPI: 4′,6-diamidino-2-phenylindole, blue

DFO: Desferrioxamine

DPBS: Dulbecco's Phosphate-Buffered Saline

DPD: Daprodustat

ECM: Extracellular matrix

EMT: Epithelial-to-mesenchymal transition

ER: Endoplasmic reticulum

ESRD: End-stage renal disease

FIH1: Factor inhibiting HIF1

GLUT1: Glucose transporter 1

HG: High glucose

HIF: Hypoxia inducible factor

HuLECs: Human Lens epithelial cells

LDHA: Lactate dehydrogenase A

LECs: Lens epithelial cells

MGP: Matrix Gla Proteins

Msx2: Msh homebox2

MTT: 3-[4,5-dimethylthiazol-2-yl]-2,5- diphenyltetrazolium bromide

NG: Normal glucose

OCN: Osteocalcin

OM: Osteogenic media

OPN: osteopontin

PDK4: Pyruvate dehydrogenase kinase 4

PFA: Paraformaldehyde

PHD: Prolyl hydroxylases

PPi: inorganic pyrophosphate

PXE: Pseudoxanthoma elasticum

RAGE: Receptor of Advanced glycation end productc

ROS: Reactive oxygen species

Runx2: Runt-related transcription factor 2

Sox9: Sry-related HMG box-9

T2D: Type 2 diabetes

VC: Vascular calcification

VEGFA: Vascular endothelial growth factor A

VHL: Von Hipple-Lindau

VICs: Valvular interstitial cells

VSMCs: Vascular smooth muscle cells

9. Acknowledgement

First, I wish to thank my family, especially my mother for her endless love and support. And my friends for their encouragement and emotional support, my lovely supervisor, Dr Viktoria Jeney, for her guidance and inspiration, and my colleagues Enikő Balogh, Andrea, Dávid Csiki Gréta Lente, and Arpan Chowdhury. Without their generous help, teaching and guidance, this work would not have been possible.

I would also like to thank István Balogh the head of the doctoral school, and András Mádi the secretary of the doctoral school of Molecular, Cellular and Immune Biology, for their support to our group.

I am thankful to the Stipendium Hungaricum Foundation for the financial support provided through their scholarship.

10. References

1. Budoff MJ, Shaw LJ, Liu ST, Weinstein SR, Tseng PH, Flores FR, et al. Long-term prognosis associated with coronary calcification: observations from a registry of 25,253 patients. J Am Coll Cardiol. 2007;49(18):1860–70.
2. Chander S, Gordon P. Soft tissue and subcutaneous calcification in connective tissue diseases. Curr Opin Rheumatol. 2012;24(2):158–64.
3. Senba M, Kawai K, Mori N. Pathogenesis of metastatic calcification and acute pancreatitis in adult T-cell leukemia under hypercalcemic state. Leuk Res Treatment. 2012;2012.
4. Karwowski W, Naumnik B, Szczepański M, Myśliwiec M. The mechanism of vascular calcification–a systematic review. Med Sci Monit. 2012;18(1):RA1.
5. De Vilder EYG, Vanakker OM. From variome to phenome: Pathogenesis, diagnosis and management of ectopic mineralization disorders. World Journal of Clinical Cases: WJCC. 2015;3(7):556.
6. Bourne LE, Wheeler-Jones CPD, Orriss IR. Regulation of mineralisation in bone and vascular tissue: A comparative review. Journal of Endocrinology. 2021;248(2):R51–65.
7. Singh A, Tandon S, Tandon C. An update on vascular calcification and potential therapeutics. Mol Biol Rep. 2021;48(1):887–96.
8. Mundy GR, Martin TJ. Physiology and pharmacology of bone. Springer; 1993.
9. Fagerholm P, Philipson B, Carlstrom D. Calcification in the human lens. Curr Eye Res. 1981;1(11):629–33.
10. Pak CYC. Etiology and treatment of urolithiasis. American journal of kidney diseases. 1991;18(6):624–37.
11. Rocha-Singh KJ, Zeller T, Jaff MR. Peripheral arterial calcification: prevalence, mechanism, detection, and clinical implications. Catheterization and Cardiovascular Interventions. 2014;83(6):E212–20.
12. Shanahan CM, Crouthamel MH, Kapustin A, Giachelli CM. Arterial calcification in chronic kidney disease: key roles for calcium and phosphate. Circ Res. 2011;109(6):697–711.
13. Rutsch F, Nitschke Y, Terkeltaub R. Genetics in arterial calcification: pieces of a puzzle and cogs in a wheel. Circ Res. 2011;109(5):578–92.
14. Thompson RC, Allam AH, Lombardi GP, Wann LS, Sutherland ML, Sutherland JD, et al. Atherosclerosis across 4000 years of human history: the Horus study of four ancient populations. The lancet. 2013;381(9873):1211–22.
15. Amann K. Media calcification and intima calcification are distinct entities in chronic kidney disease. Clinical Journal of the American Society of Nephrology. 2008;3(6):1599–605.

16. Schlotter F, Halu A, Goto S, Blaser MC, Body SC, Lee LH, et al. Spatiotemporal multi-omics mapping generates a molecular atlas of the aortic valve and reveals networks driving disease. Circulation. 2018;138(4):377–93.

17. Bäck M, Aranyi T, Cancela ML, Carracedo M, Conceição N, Leftheriotis G, et al. Endogenous calcification inhibitors in the prevention of vascular calcification: a consensus statement from the COST action EuroSoftCalcNet. Front Cardiovasc Med. 2019;5:196.

18. Small A, Kiss D, Giri J, Anwaruddin S, Siddiqi H, Guerraty M, et al. Biomarkers of calcific aortic valve disease. Arterioscler Thromb Vasc Biol. 2017;37(4):623–32.

19. Neven E, De Schutter TM, De Broe ME, D'haese PC. Cell biological and physicochemical aspects of arterial calcification. Kidney Int. 2011;79(11):1166–77.

20. Hortells L, Sur S, St. Hilaire C. Cell phenotype transitions in cardiovascular calcification. Front Cardiovasc Med. 2018;5:27.

21. Lin ME, Chen T, Leaf EM, Speer MY, Giachelli CM. Runx2 expression in smooth muscle cells is required for arterial medial calcification in mice. Am J Pathol. 2015;185(7):1958–69.

22. Shao JS, Cheng SL, Pingsterhaus JM, Charlton-Kachigian N, Loewy AP, Towler DA. Msx2 promotes cardiovascular calcification by activating paracrine Wnt signals. J Clin Invest. 2005;115(5):1210–20.

23. Lee HY, Lim S, Park S. Role of inflammation in arterial calcification. Korean Circ J. 2021;51(2):114.

24. Rao Z, Zheng Y, Xu L, Wang Z, Zhou Y, Chen M, et al. Endoplasmic reticulum stress and pathogenesis of vascular calcification. Front Cardiovasc Med. 2022;9:918056.

25. Rennenberg MW, Kessels AGH, Schurgers LJ, Van Engelshoven JMA, De Leeuw PW, Kroon AA. Vascular calcifi cations as a marker of increased cardiovascular risk: A meta-analysis. Vascular Health and Risk Management. 2009.

26. Smith ER, Holt SG, Hewitson TD. αKlotho–FGF23 interactions and their role in kidney disease: a molecular insight. Cellular and molecular life sciences. 2019;76(23):4705–24.

27. Paloian NJ, Giachelli CM. A current understanding of vascular calcification in CKD. American Journal of Physiology-Renal Physiology. 2014;307(8):F891–900.

28. Yamada S, Giachelli CM. Vascular calcification in CKD-MBD: Roles for phosphate, FGF23, and Klotho. Bone. 2017;100:87–93.

29. Adeney KL, Siscovick DS, Ix JH, Seliger SL, Shlipak MG, Jenny NS, et al. Association of serum phosphate with vascular and valvular calcification in moderate CKD. Journal of the American Society of Nephrology. 2009;20(2):381–7.

30. Balogh E, Tóth A, Méhes G, Trencsényi G, Paragh G, Jeney V. Hypoxia Triggers Osteochondrogenic Differentiation of Vascular Smooth Muscle Cells in an HIF-1

(Hypoxia-Inducible Factor 1)-Dependent and Reactive Oxygen Species-Dependent Manner. Arterioscler Thromb Vasc Biol. 2019 Jun 1;39(6):1088–99.

31. Cozzolino M, Ciceri P, Galassi A, Mangano M, Carugo S, Capelli I, et al. The key role of phosphate on vascular calcification. Vol. 11, Toxins. MDPI AG; 2019.

32. Villa-Bellosta R, Bogaert YE, Levi M, Sorribas V. Characterization of phosphate transport in rat vascular smooth muscle cells: implications for vascular calcification. Arterioscler Thromb Vasc Biol. 2007;27(5):1030–6.

33. Voelkl J, Lang F, Eckardt KU, Amann K, Kuro-o M, Pasch A, et al. Signaling pathways involved in vascular smooth muscle cell calcification during hyperphosphatemia. Cellular and Molecular Life Sciences. Birkhauser Verlag AG; 2019.

34. Giachelli CM. The emerging role of phosphate in vascular calcification. Kidney Int. 2009 May;75(9):890–7.

35. Proudfoot D, Skepper JN, Hegyi L, Bennett MR, Shanahan CM, Weissberg PL. Apoptosis regulates human vascular calcification in vitro: evidence for initiation of vascular calcification by apoptotic bodies. Circ Res. 2000;87(11):1055–62.

36. Clarke MCH, Littlewood TD, Figg N, Maguire JJ, Davenport AP, Goddard M, et al. Chronic apoptosis of vascular smooth muscle cells accelerates atherosclerosis and promotes calcification and medial degeneration. Circ Res. 2008;102(12):1529–38.

37. Kapustin AN, Davies JD, Reynolds JL, McNair R, Jones GT, Sidibe A, et al. Calcium regulates key components of vascular smooth muscle cell–derived matrix vesicles to enhance mineralization. Circ Res. 2011;109(1):e1–12.

38. Tóth A, Balogh E, Jeney V. Regulation of vascular calcification by reactive oxygen species. Antioxidants. 2020;9(10):963.

39. Giachelli CM. Inducers and inhibitors of biomineralization: lessons from pathological calcification. Orthod Craniofac Res. 2005;8(4):229–31.

40. Magliano DJ, Boyko EJ, committee =IDF Diabetes Atlas 10th edition scientific. IDF DIABETES ATLAS [Internet]. 10th ed. International Diabetes Federation, Brussels; 2021. (IDF Diabetes Atlas). Available from: http://europepmc.org/abstract/MED/35914061

41. Ghosh S, Luo D, He W, Chen J, Su X, Huang H. Diabetes and calcification: The potential role of anti-diabetic drugs on vascular calcification regression. Vol. 158, Pharmacological Research. Academic Press; 2020.

42. Yahagi K, Kolodgie FD, Lutter C, Mori H, Romero ME, Finn A V., et al. Pathology of human coronary and carotid artery atherosclerosis and vascular calcification in diabetes mellitus. Vol. 37, Arteriosclerosis, Thrombosis, and Vascular Biology. Lippincott Williams and Wilkins; 2017. p. 191–204.

43. Raggi P, Shaw LJ, Berman DS, Callister TQ. Prognostic value of coronary artery calcium screening in subjects with and without diabetes. J Am Coll Cardiol. 2004 May 5;43(9):1663–9.

44. Stabley JN, Towler DA. Arterial calcification in diabetes mellitus: preclinical models and translational implications. Arterioscler Thromb Vasc Biol. 2017;37(2):205–17.

45. Raaz U, Schellinger IN, Chernogubova E, Warnecke C, Kayama Y, Penov K, et al. Transcription factor Runx2 promotes aortic fibrosis and stiffness in type 2 diabetes mellitus. Circ Res. 2015;117(6):513–24.

46. Liu H, Huang LH, Sun XY, Ouyang JM. High-phosphorus environment promotes calcification of A7R5 cells induced by hydroxyapatite nanoparticles. Materials Science and Engineering: C. 2020;107:110228.

47. Bardeesi ASA, Gao J, Zhang K, Yu S, Wei M, Liu P, et al. A novel role of cellular interactions in vascular calcification. J Transl Med. 2017;15:1–8.

48. Oguntibeju OO. Type 2 diabetes mellitus, oxidative stress and inflammation: examining the links. Int J Physiol Pathophysiol Pharmacol. 2019;11(3):45.

49. Butkowski EG, Jelinek HF. Hyperglycaemia, oxidative stress and inflammatory markers. Redox Report [Internet]. 2017 Nov 2;22(6):257–64. Available from: https://doi.org/10.1080/13510002.2016.1215643

50. Wei Q, Ren X, Jiang Y, Jin H, Liu N, Li J. Advanced glycation end products accelerate rat vascular calcification through RAGE/oxidative stress. BMC Cardiovasc Disord. 2013;13:1–10.

51. Kay AM, Simpson CL, Stewart JA. The role of AGE/RAGE signaling in diabetes-mediated vascular calcification. J Diabetes Res. 2016;2016.

52. Ma WQ, Liu NF. Research update on the AGE/RAGE signaling mediated vascular calcification in diabetes. Zhonghua Xin Xue Guan Bing Za Zhi. 2018;46(9):745–50.

53. Sun XJ, Liu NF. Diabetic mellitus, vascular calcification and hypoxia: A complex and neglected tripartite relationship. Cell Signal. 2022;91:110219.

54. Shi L, Yu X, Yang H, Wu X. Advanced glycation end products induce human corneal epithelial cells apoptosis through generation of reactive oxygen species and activation of JNK and p38 MAPK pathways. PLoS One. 2013;8(6):e66781.

55. Bierhaus A, Nawroth PP. Multiple levels of regulation determine the role of the receptor for AGE (RAGE) as common soil in inflammation, immune responses and diabetes mellitus and its complications. Diabetologia. 2009;52:2251–63.

56. Rai V, Maldonado AY, Burz DS, Reverdatto S, Schmidt AM, Shekhtman A. Signal Transduction in Receptor for Advanced Glycation End Products (RAGE). Journal of Biological Chemistry. 2012;287(7):5133–44.

57. A Chistiakov D, A Sobenin I, N Orekhov A, V Bobryshev Y. Mechanisms of medial arterial calcification in diabetes. Curr Pharm Des. 2014;20(37):5870–83.

58. Imtiaz R, Hawken S, McCormick BB, Leung S, Hiremath S, Zimmerman DL. Diabetes mellitus and younger age are risk factors for hyperphosphatemia in peritoneal dialysis patients. Nutrients. 2017;9(2):152.

59. Shang D, Xie Q, Ge X, Yan H, Tian J, Kuang D, et al. Hyperphosphatemia as an independent risk factor for coronary artery calcification progression in peritoneal dialysis patients. BMC Nephrol. 2015;16:1–9.

60. Bronzino JD. Biomedical Engineering Handbook 2. Vol. 2. Springer Science & Business Media; 2000.

61. Moss C. Neuroethological studies of cognitive and perceptual processes. Routledge; 2018.

62. Seyahi N, Altiparmak MR, Kahveci A, Yetik H, Kanberoglu K, Serdengecti K, et al. Association of conjunctival and corneal calcification with vascular calcification in dialysis patients. American journal of kidney diseases. 2005;45(3):550–6.

63. Sun W, Sun M, Zhang M, Liu Y, Lin X, Zhao S, et al. Correlation between conjunctival and corneal calcification and cardiovascular calcification in patients undergoing maintenance hemodialysis. Hemodialysis International. 2015;19(2):270–8.

64. TURGUT B, ERDOGAN H, Emre O, ERŞAN İ. Senile Scleral Plaque Evaluation With Optical Coherence Tomography. Tıp Fakültesi Klinikleri Dergisi. 2023;5(2–3):93–6.

65. Samaka RM, Al-Madhani A, Hussian SO. Subepidermal calcified nodule in upper eyelid: A case report and review of the literature. Oman J Ophthalmol. 2015;8(1):56–8.

66. Tan ACS, Pilgrim MG, Fearn S, Bertazzo S, Tsolaki E, Morrell AP, et al. Calcified nodules in retinal drusen are associated with disease progression in age-related macular degeneration. Sci Transl Med. 2018;10(466):eaat4544.

67. D'Marco L, Lima-Martínez M, Karohl C, Chacín M, Bermúdez V. Pseudoxanthoma elasticum: an interesting model to evaluate chronic kidney disease-like vascular damage without renal disease. Kidney Diseases. 2020;6(2):92–7.

68. Yang G, Mack H, Harraka P, Colville D, Savige J. Ocular manifestations of the genetic renal tubulopathies. Ophthalmic Genet. 2023;44(6):515–29.

69. Kachewar SG, KulKaRni DS. An imaging review of intra-ocular calcifications. J Clin Diagn Res. 2014;8(1):203.

70. Thulasidas M, Amin H. Ocular evaluation in patients with chronic kidney disease-A hospital based study. Open Access J Ophthalmol. 2018;3.

71. Wong CW, Wong TY, Cheng CY, Sabanayagam C. Kidney and eye diseases: common risk factors, etiological mechanisms, and pathways. Kidney Int. 2014;85(6):1290–302.

72. Mittl R, Galin MA, Opperman W, Camerini-Davalos RA, Spiro D. Corneal calcification in spontaneously diabetic mice. Invest Ophthalmol Vis Sci. 1970;9(2):137–45.

73. Hsiao CH, Chao A, Chu SY, Lin KK, Yeung L, Lin-Tan DT, et al. Association of severity of conjunctival and corneal calcification with all-cause 1-year mortality in maintenance haemodialysis patients. Nephrology Dialysis Transplantation. 2011;26(3):1016–23.

74. Klaassen-Broekema N, Van Bijsterveld OP. Limbal and corneal calcification in patients with chronic renal failure. British journal of ophthalmology. 1993;77(9):569–71.

75. Porter R, Crombie AL. Corneal and conjunctival calcification in chronic renal failure. Br J Ophthalmol. 1973;57(5):339.

76. Duque EJ, Elias RM, Moysés RMA. Parathyroid hormone: a uremic toxin. Toxins (Basel). 2020;12(3):189.

77. Weng SF, Jan RL, Chang C, Wang JJ, Su SB, Huang CC, et al. Risk of Band Keratopathy in Patients with End-Stage Renal Disease. Scientif [Internet]. 2016;6(1):28675. Available from: https://doi.org/10.1038/srep28675

78. Jhanji V, Rapuano CJ, Vajpayee RB. Corneal calcific band keratopathy. Curr Opin Ophthalmol [Internet]. 2011;22(4). Available from: https://journals.lww.com/co-ophthalmology/fulltext/2011/07000/corneal_calcific_band_keratopathy.14.aspx

79. Moisseiev E, Gal A, Addadi L, Caspi D, Shemesh G, Michaeli A. Acute calcific band keratopathy: Case report and literature review. J Cataract Refract Surg [Internet]. 2013;39(2). Available from: https://journals.lww.com/jcrs/fulltext/2013/02000/acute_calcific_band_keratopathy__case_report_and.22.aspx

80. O'Connor GR. CALCIFIC BAND KERATOPATHY*. 1972.

81. Nongpiur ME, Wong TY, Sabanayagam C, Lim SC, Tai ES, Aung T. Chronic Kidney Disease and Intraocular Pressure: The Singapore Malay Eye Study. Ophthalmology [Internet]. 2010;117(3):477–83. Available from: https://www.sciencedirect.com/science/article/pii/S0161642009008379

82. Patel D V, Snead MP, Satchi K. Retinal arteriolar calcification in a patient with chronic renal failure. British journal of ophthalmology. 2002;86(9):1063.

83. Risseeuw S, Pilgrim MG, Bertazzo S, Brown CN, Csincsik L, Fearn S, et al. Bruch's Membrane Calcification in Pseudoxanthoma Elasticum: Comparing Histopathology and Clinical Imaging. Ophthalmology Science. 2024 Mar 1;4(2).

84. Thompson RB, Reffatto V, Bundy JG, Kortvely E, Flinn JM, Lanzirotti A, et al. Identification of hydroxyapatite spherules provides new insight into subretinal pigment epithelial deposit formation in the aging eye. Proceedings of the National Academy of Sciences. 2015;112(5):1565–70.

85. Pilgrim MG, Marouf S, Fearn S, Csincsik L, Kortvely E, Knowles JC, et al. Characterization of calcium phosphate spherical particles in the subretinal pigment epithelium–basal lamina space in aged human eyes. Ophthalmology Science. 2021;1(3):100053.

86. Hegde KR, Ray K, Szmacinski H, Sorto S, Puche AC, Lengyel I, et al. Two-Photon Excited Fluorescence Lifetime Imaging of Tetracycline-Labeled Retinal Calcification. Sensors. 2023 Jul 1;23(14).

87. Sarks SH. Ageing and degeneration in the macular region: a clinico-pathological study. British Journal of Ophthalmology. 1976;60(5):324–41.

88. Bourne RRA, Jonas JB, Flaxman SR, Keeffe J, Leasher J, Naidoo K, et al. Prevalence and causes of vision loss in high-income countries and in Eastern and Central Europe: 1990–2010. British Journal of Ophthalmology. 2014;98(5):629–38.

89. Bhutto I, Lutty G. Understanding age-related macular degeneration (AMD): relationships between the photoreceptor/retinal pigment epithelium/Bruch's membrane/choriocapillaris complex. Mol Aspects Med. 2012;33(4):295–317.

90. Bergen AAB, Plomp AS, Schuurman EJ, Terry S, Breuning M, Dauwerse H, et al. Mutations in ABCC6 cause pseudoxanthoma elasticum. Nat Genet. 2000;25(2):228–31.

91. Le Saux O, Urban Z, Tschuch C, Csiszar K, Bacchelli B, Quaglino D, et al. Mutations in a gene encoding an ABC transporter cause pseudoxanthoma elasticum. Nat Genet. 2000;25(2):223–7.

92. Ramrattan RS, van der Schaft TL, Mooy CM, De Bruijn WC, Mulder PG, De Jong PT. Morphometric analysis of Bruch's membrane, the choriocapillaris, and the choroid in aging. Invest Ophthalmol Vis Sci. 1994;35(6):2857–64.

93. Jansen RS, Küçükosmanoğlu A, De Haas M, Sapthu S, Otero JA, Hegman IEM, et al. ABCC6 prevents ectopic mineralization seen in pseudoxanthoma elasticum by inducing cellular nucleotide release. Proceedings of the National Academy of Sciences. 2013;110(50):20206–11.

94. Sridhar MS. Anatomy of cornea and ocular surface. Vol. 66, Indian Journal of Ophthalmology. Medknow Publications; 2018. p. 190–4.

95. Spemann H. Ueber korrelationen in der entwicklung des auges. Verh Anat Ges. 1901;15:61–79.

96. Renwick JH, Lawler SD. Probable linkage between a congenital cataract locus and the Duffy blood group locus. Ann Hum Genet. 1963;27(1):67–76.

97. Wistow GJ, Piatigorsky J. Lens crystallins: the evolution and expression of proteins for a highly specialized tissue. Annu Rev Biochem. 1988;57(1):479–504.

98. Hejtmancik JF, Shiels A. Overview of the Lens. In: Progress in Molecular Biology and Translational Science. Elsevier B.V.; 2015. p. 119–27.

99. Danysh BP, Duncan MK. The lens capsule. Exp Eye Res. 2009;88(2):151–64.

100. Vrensen G. Aging of the human eye lens—a morphological point of view. Comp Biochem Physiol A Physiol. 1995;111(4):519–32.

101. Michael R, van Marle J, Vrensen GFJM, van den Berg TJTP. Changes in the refractive index of lens fibre membranes during maturation–impact on lens transparency. Exp Eye Res. 2003;77(1):93–9.

102. Xiao W, Chen X, Li W, Ye S, Wang W, Luo L, et al. Quantitative analysis of injury-induced anterior subcapsular cataract in the mouse: a model of lens epithelial cells proliferation and epithelial-mesenchymal transition. Sci Rep. 2015;5(1):8362.

103. De Iongh RU, Wederell E, Lovicu FJ, McAvoy JW. Transforming growth factor-β-induced epithelial-mesenchymal transition in the lens: a model for cataract formation. Cells Tissues Organs. 2005;179(1–2):43–55.

104. Balogh E, Tóth A, Tolnai E, Bodó T, Bányai E, Szabó DJ, et al. Osteogenic differentiation of human lens epithelial cells might contribute to lens calcification. Biochim Biophys Acta Mol Basis Dis. 2016 Sep 1;1862(9):1724–31.

105. Boix-Lemonche G, Nagymihaly RM, Lumi X, Petrovski G. The human lens is capable of trilineage differentiation towards osteo-, chondro-, and adipogenesis—a model for studying cataract pathogenesis. Front Bioeng Biotechnol. 2023;11:1164795.

106. Cicinelli MV, Buchan JC, Nicholson M, Varadaraj V, Khanna RC. Cataracts. The Lancet. 2023;401(10374):377–89.

107. Hashemi H, Pakzad R, Yekta A, Aghamirsalim M, Pakbin M, Ramin S, et al. Global and regional prevalence of age-related cataract: a comprehensive systematic review and meta-analysis. Eye. 2020;34(8):1357–70.

108. Robman L, Taylor H. External factors in the development of cataract. Eye. 2005;19(10):1074–82.

109. Asbell PA, Dualan I, Mindel J, Brocks D, Ahmad M, Epstein S. Age-related cataract. The Lancet. 2005;365(9459):599–609.

110. Klein R, Klein BEK. The prevalence of age-related eye diseases and visual impairment in aging: current estimates. Invest Ophthalmol Vis Sci. 2013;54(14):ORSF5–13.

111. Allen D, Vasavada A. Cataract and surgery for cataract. Bmj. 2006;333(7559):128–32.

112. Spector A. Aggregation of a-crystallin and its possible relationship to cataract formation. Isr J Med Sci. 1972 Aug;8(8):1577–82.

113. Wada E, Sugiura T, Nakamura H, Tsumita T. Studies on lens proteins of mice with hereditary cataract. I. Comparative studies on the chemical and immunochemical properties of the soluble proteins of cataractous and normal mouse lenses. BBA - Protein Structure. 1981 Feb 27;667(2):251–9.

114. Depeiges A, Dufaure JP. Major proteins secreted by the epididymis of Lacerta vivipara. Identification by electrophoresis of soluble proteins. BBA - Protein Structure. 1981 Feb 27;667(2):260–6.

115. Moreau KL, King JA. Protein misfolding and aggregation in cataract disease and prospects for prevention. Trends Mol Med. 2012 May;18(5):273–82.

116. Drinkwater JJ, Davis WA, Davis TME. A systematic review of risk factors for cataract in type 2 diabetes. Diabetes Metab Res Rev. 2019;35(1):e3073.

117. Feldman-Billard S, Dupas B. Eye disorders other than diabetic retinopathy in patients with diabetes. Diabetes Metab. 2021;47(6):101279.

118. Keith B, Johnson RS, Simon MC. HIF1α and HIF2α: sibling rivalry in hypoxic tumour growth and progression. Nat Rev Cancer. 2012;12(1):9–22.

119. Semenza GL. Hypoxia-inducible factors in physiology and medicine. Cell. 2012;148(3):399–408.

120. Markolovic S, Wilkins SE, Schofield CJ. Protein hydroxylation catalyzed by 2-oxoglutarate-dependent oxygenases. Journal of Biological Chemistry. 2015;290(34):20712–22.

121. Kaelin WG, Ratcliffe PJ. Oxygen sensing by metazoans: the central role of the HIF hydroxylase pathway. Mol Cell. 2008;30(4):393–402.

122. Lando D, Peet DJ, Whelan DA, Gorman JJ, Whitelaw ML. Asparagine hydroxylation of the HIF transactivation domain: a hypoxic switch. Science (1979). 2002;295(5556):858–61.

123. Semenza GL. HIF-1: upstream and downstream of cancer metabolism. Curr Opin Genet Dev. 2010;20(1):51–6.

124. Zhu Y, Wang Y, Jia Y, Xu J, Chai Y. Roxadustat promotes angiogenesis through HIF-1α/VEGF/VEGFR2 signaling and accelerates cutaneous wound healing in diabetic rats. Wound repair and regeneration. 2019;27(4):324–34.

125. Ma WQ, Sun XJ, Zhu Y, Liu NF. PDK4 promotes vascular calcification by interfering with autophagic activity and metabolic reprogramming. Cell Death Dis. 2020;11(11):991.

126. Li G, Lu W hua, Ai R, Yang J hong, Chen F, Tang Z zhi. The relationship between serum hypoxia-inducible factor 1α and coronary artery calcification in asymptomatic type 2 diabetic patients. Cardiovasc Diabetol. 2014;13:1–8.

127. Han X, Wang XL, Li Q, Dong XX, Zhang JS, Yan QC. HIF-1α SUMOylation affects the stability and transcriptional activity of HIF-1α in human lens epithelial cells. Graefe's Archive for Clinical and Experimental Ophthalmology. 2015;253:1279–90.

128. Gao W, Ferguson G, Connell P, Walshe T, Murphy R, Birney YA, et al. High glucose concentrations alter hypoxia-induced control of vascular smooth muscle cell growth via a HIF-1α-dependent pathway. J Mol Cell Cardiol. 2007 Mar;42(3):609–19.

129. Fuhrmann DC, Brüne B. Mitochondrial composition and function under the control of hypoxia. Redox Biol. 2017;12:208–15.

130. Zhu Y, Ma WQ, Han XQ, Wang Y, Wang X, Liu NF. Advanced glycation end products accelerate calcification in VSMCs through HIF-1α/PDK4 activation and suppress glucose metabolism. Sci Rep. 2018;8(1):13730.

131. Copur S, Ucku D, Cozzolino M, Kanbay M. Hypoxia-inducible factor signaling in vascular calcification in chronic kidney disease patients. Vol. 35, Journal of Nephrology. Springer Science and Business Media Deutschland GmbH; 2022. p. 2205–13.

132. Li J, Yang YL, Li LZ, Zhang L, Liu Q, Liu K, et al. Succinate accumulation impairs cardiac pyruvate dehydrogenase activity through GRP91-dependent and independent signaling pathways: Therapeutic effects of ginsenoside Rb1. Biochimica et Biophysica Acta (BBA)-Molecular Basis of Disease. 2017;1863(11):2835–47.

133. Lee SJ, Jeong JY, Oh CJ, Park S, Kim JY, Kim HJ, et al. Pyruvate dehydrogenase kinase 4 promotes vascular calcification via SMAD1/5/8 phosphorylation. Sci Rep. 2015;5(1):16577.

134. Packer M. Mutual antagonism of hypoxia-inducible factor isoforms in cardiac, vascular, and renal disorders. Basic to Translational Science. 2020;5(9):961–8.

135. Elbatreek MH, Pachado MP, Cuadrado A, Jandeleit-Dahm K, Schmidt HHHW. Reactive oxygen comes of age: mechanism-based therapy of diabetic end-organ damage. Trends in Endocrinology & Metabolism. 2019;30(5):312–27.

136. Iacobini C, Vitale M, Haxhi J, Pesce C, Pugliese G, Menini S. Mutual Regulation between Redox and Hypoxia-Inducible Factors in Cardiovascular and Renal Complications of Diabetes. Vol. 11, Antioxidants. MDPI; 2022.

137. Guzy RD, Hoyos B, Robin E, Chen H, Liu L, Mansfield KD, et al. Mitochondrial complex III is required for hypoxia-induced ROS production and cellular oxygen sensing. Cell Metab. 2005;1(6):401–8.

138. Brownlee M. The pathobiology of diabetic complications: a unifying mechanism. Diabetes. 2005;54(6):1615–25.

139. Williams MC, Murchison JT, Edwards LD, Agustí A, Bakke P, Calverley PMA, et al. Coronary artery calcification is increased in patients with COPD and associated with increased morbidity and mortality. Thorax. 2014;69(8):718–23.

140. Green FHY, Butt JC, James AL, Carroll NG. Abnormalities of the bronchial arteries in asthma. Chest. 2006;130(4):1025–33.

141. Tachikawa R, Koyasu S, Matsumoto T, Hamada S, Azuma M, Murase K, et al. Obstructive sleep apnea and abdominal aortic calcification: is there an association independent of comorbid risk factors? Atherosclerosis. 2015;241(1):6–11.

142. Mokas S, Larivière R, Lamalice L, Gobeil S, Cornfield DN, Agharazii M, et al. Hypoxia-inducible factor-1 plays a role in phosphate-induced vascular smooth muscle cell calcification. Kidney Int. 2016 Sep 1;90(3):598–609.

143. Tóth A, Csiki DM, Nagy B, Balogh E, Lente G, Ababneh H, et al. Daprodustat Accelerates High Phosphate-Induced Calcification Through the Activation of HIF-1 Signaling. Front Pharmacol. 2022 Feb 7;13.

144. Tintut Y, Alfonso Z, Saini T, Radcliff K, Watson K, Boström K, et al. Multilineage potential of cells from the artery wall. Circulation. 2003;108(20):2505–10.

145. Ang MJ, Afshari NA. Cataract and systemic disease: A review. Clin Exp Ophthalmol. 2021;49(2):118–27.

146. Klein BEK, Klein R, Moss SE. Prevalence of cataracts in a population-based study of persons with diabetes mellitus. Ophthalmology. 1985;92(9):1191–6.

147. Klein BEK, Klein R, Lee KE. Diabetes, cardiovascular disease, selected cardiovascular disease risk factors, and the 5-year incidence of age-related cataract and progression of lens opacities: the Beaver Dam Eye Study. Am J Ophthalmol. 1998;126(6):782–90.

148. Rowe N, Mitchell P, Cumming RG, Wans JJ. Diabetes, fasting blood glucose and age-related cataract: the Blue Mountains Eye Study. Ophthalmic Epidemiol. 2000;7(2):103–14.

149. Chitra PS, Chaki D, Boiroju NK, Mokalla TR, Gadde AK, Agraharam SG, et al. Status of oxidative stress markers, advanced glycation index, and polyol pathway in age-related cataract subjects with and without diabetes. Exp Eye Res. 2020;200:108230.

150. Perry RE, Swamy MS, Abraham EC. Progressive changes in lens crystallin glycation and high-molecular-weight aggregate formation leading to cataract development in streptozotocin-diabetic rats. Exp Eye Res. 1987;44(2):269–82.

151. Van Boekel MAM, Hoenders HJ. Glycation of crystalline in lenses from aging and diabetic individuals. FEBS Lett. 1992;314(1):1–4.

152. Lee AYW, Chung SSM. Contributions of polyol pathway to oxidative stress in diabetic cataract. The FASEB journal. 1999;13(1):23–30.

153. Li H, Xu L, Song H. Mir-29a alleviates high glucose-induced inflammation and mitochondrial dysfunction via modulation of il-6/stat3 in diabetic cataracts. Curr Eye Res. 2021;46(9):1325–32.

154. Lian L, Le Z, Wang Z, Chen Y ao, Jiao X, Qi H, et al. SIRT1 Inhibits High Glucose–Induced TXNIP/NLRP3 Inflammasome Activation and Cataract Formation. Invest Ophthalmol Vis Sci. 2023;64(3):16.

155. Ma Z, Liu J, Li J, Jiang H, Kong J. Klotho ameliorates the onset and progression of cataract via suppressing oxidative stress and inflammation in the lens in streptozotocin-induced diabetic rats. Int Immunopharmacol. 2020;85:106582.

156. Chiang SY, Horng CT, Lee WH, Chang CJ. Calcified cataractous lens. J Cataract Refract Surg. 2004;30(7):1586–9.

157. CHEN K, CHENG W, LI M, YANG D, LIN S. Calcification of senile cataractous lens determined by Fourier transform infrared (FTIR) and Raman microspectroscopies. J Microsc. 2005;219(1):36–41.

158. Lin SY, Chen KH, Lin CC, Cheng WT, Li MJ. Spectral analysis and comparison of mineral deposits forming in opacified intraocular lens and senile cataractous lens. Spectrochim Acta A Mol Biomol Spectrosc. 2010;77(3):703–8.

159. Fagerholm P, Lundevall E, Trocmé S, Wroblewski R. Human and experimental lens repair and calcification. Exp Eye Res. 1986;43(6):965–72.

160. Sayin N, Kara N, Pekel G. Ocular complications of diabetes mellitus. World J Diabetes. 2015;6(1):92.

161. Mackenzie NCW, E MacRae V. The role of cellular senescence during vascular calcification: a key paradigm in aging research. Curr Aging Sci. 2011;4(2):128–36.

162. Virmani R, Joner M, Sakakura K. Recent highlights of ATVB: calcification. Arterioscler Thromb Vasc Biol. 2014;34(7):1329–32.

163. Van Esch H, Agarwal AK, Debeer P, Fryns JP, Garg A. A homozygous mutation in the lamin A/C gene associated with a novel syndrome of arthropathy, tendinous calcinosis, and progeroid features. J Clin Endocrinol Metab. 2006;91(2):517–21.

164. Hough TA, Bogani D, Cheeseman MT, Favor J, Nesbit MA, Thakker R V, et al. Activating calcium-sensing receptor mutation in the mouse is associated with cataracts and ectopic calcification. Proceedings of the National Academy of Sciences. 2004;101(37):13566–71.

165. Fryns JP, Dumoulin M, Hens G. Progeroid syndrome with facial teleangiectatic erythema, posterior subcapsular cataracts, calcification of basal ganglia and atrium septum defect type 2. Genet Couns. 1999;10(4):395–8.

166. Sonmez FM, Celep F, Ugur SA. Severe form of Cockayne syndrome with varying clinical presentation and no photosensitivity in a family. J Child Neurol. 2006;21(4):333–7.

167. Nikolov IG, Mozar A, Drüeke TB, Massy ZA. Impact of disturbances of calcium and phosphate metabolism on vascular calcification and clinical outcomes in patients with chronic kidney disease. Blood Purif. 2009;27(4):350–9.

168. Giachelli CM, Jono S, Shioi A, Nishizawa Y, Mori K, Morii H. Vascular calcification and inorganic phosphate. American journal of kidney diseases. 2001;38(4):S34–7.

169. Mehrotra R, Budoff M, Christenson P, Ipp E, Takasu J, Gupta A, et al. Determinants of coronary artery calcification in diabetics with and without nephropathy. Kidney Int. 2004;66(5):2022–31.

170. Chen NX, Duan D, O'Neill KD, Moe SM. High glucose increases the expression of Cbfa1 and BMP-2 and enhances the calcification of vascular smooth muscle cells. Nephrology Dialysis Transplantation. 2006 Dec 1;21(12):3435–42.

171. Moe SM, O'Neill KD, Duan D, Ahmed S, Chen NX, Leapman SB, et al. Medial artery calcification in ESRD patients is associated with deposition of bone matrix proteins. Kidney Int. 2002;61(2):638–47.

172. Son DJ, Jung YY, Seo YS, Park H, Lee DH, Kim S, et al. Interleukin-32α inhibits endothelial inflammation, vascular smooth muscle cell activation, and atherosclerosis by upregulating Timp3 and Reck through suppressing microRNA-205 biogenesis. Theranostics. 2017;7(8):2186–203.

173. Linton MF, Babaev VR, Huang J, Linton EF, Tao H, Yancey PG. Macrophage apoptosis and efferocytosis in the pathogenesis of atherosclerosis. Vol. 80, Circulation Journal. Japanese Circulation Society; 2016. p. 2259–68.

174. Yao L, Chandra S, Toque HA, Bhatta A, Rojas M, Caldwell RB, et al. Prevention of diabetes-induced arginase activation and vascular dysfunction by Rho kinase (ROCK) knockout. Cardiovasc Res [Internet]. 2013 Mar 1;97(3):509–19. Available from: https://doi.org/10.1093/cvr/cvs371

175. Lynch MP, Capparelli C, Stein JL, Stein GS, Lian JB. Apoptosis during bone-like tissue development in vitro. J Cell Biochem. 1998 Jan 1;68(1):31–49.

176. Kim KM. Apoptosis and Calcification [Internet]. Vol. 9, Scanning Microscopy. 1995. Available from: https://digitalcommons.usu.edu/microscopyAvailableat:https://digitalcommons.usu.edu/microscopy/vol9/iss4/19

177. Kockx MM, Muhring J, Bortier H, De Meyer GRY, Jacob W. Copyrigbt C) A merican Society for Investigative Pathology Technical Advance Biotin-or Digoxigenin-Conjugated Nucleotides Bind to Matrix Vesicles in Atherosclerotic Plaques. Vol. 148, Americani Journal of Pathology. 1996.

178. Hashimoto S, Ochs RL, Rosen F, Quach J, McCabe G, Solan J, et al. Chondrocyte-derived apoptotic bodies and calcification of articular cartilage. Proceedings of the National Academy of Sciences [Internet]. 1998 Mar 17;95(6):3094–9. Available from: https://doi.org/10.1073/pnas.95.6.3094

179. Zhang J, Reedy MC, Hannun YA, Obeid LM. Inhibition of Caspases Inhibits the Release of Apoptotic Bodies: Bcl-2 Inhibits the Initiation of Formation of Apoptotic Bodies in Chemotherapeutic Agent-induced Apoptosis. Journal of Cell Biology [Internet]. 1999 Apr 5;145(1):99–108. Available from: https://doi.org/10.1083/jcb.145.1.99

180. Bi W, Deng JM, Zhang Z, Behringer RR, De Crombrugghe B. Sox9 is required for cartilage formation. Nat Genet. 1999;22(1):85–9.

181. Yoshida CA, Furuichi T, Fujita T, Fukuyama R, Kanatani N, Kobayashi S, et al. Core-binding factor β interacts with Runx2 and is required for skeletal development. Nat Genet. 2002;32(4):633–8.

182. Schinke T, Karsenty G. Transcriptional control of osteoblast differentiation and function. In: Principles of bone biology. Elsevier; 2002. p. 83–91.

183. Choi KY, Lee SW, Park MH, Bae YC, Shin HI, Nam SH, et al. Spatio-temporal expression patterns of Runx2 isoforms in early skeletogenesis. Exp Mol Med. 2002;34(6):426–33.

184. Komori T, Yagi H, Nomura S, Yamaguchi A, Sasaki K, Deguchi K, et al. Targeted disruption of Cbfa1 results in a complete lack of bone formation owing to maturational arrest of osteoblasts. Cell. 1997;89(5):755–64.

185. Otto F, Thornell AP, Crompton T, Denzel A, Gilmour KC, Rosewell IR, et al. Cbfa1, a candidate gene for cleidocranial dysplasia syndrome, is essential for osteoblast differentiation and bone development. Cell. 1997;89(5):765–71.

186. Ducy P, Zhang R, Geoffroy V, Ridall AL, Karsenty G. Osf2/Cbfa1: a transcriptional activator of osteoblast differentiation. Cell. 1997;89(5):747–54.

187. Okuda T, Van Deursen J, Hiebert SW, Grosveld G, Downing JR. AML1, the target of multiple chromosomal translocations in human leukemia, is essential for normal fetal liver hematopoiesis. Cell. 1996;84(2):321–30.

188. Sasaki K, Yagi H, Bronson RT, Tominaga K, Matsunashi T, Deguchi K, et al. Absence of fetal liver hematopoiesis in mice deficient in transcriptional coactivator core binding factor beta. Proceedings of the National Academy of Sciences. 1996;93(22):12359–63.

189. Wang Q, Stacy T, Binder M, Marin-Padilla M, Sharpe AH, Speck NA. Disruption of the Cbfa2 gene causes necrosis and hemorrhaging in the central nervous system and blocks definitive hematopoiesis. Proceedings of the National Academy of Sciences. 1996;93(8):3444–9.

190. Wang Q, Stacy T, Miller JD, Lewis AF, Gu TL, Huang X, et al. The CBFβ subunit is essential for CBFα2 (AML1) function in vivo. Cell. 1996;87(4):697–708.

191. Takeda S, Bonnamy JP, Owen MJ, Ducy P, Karsenty G. Continuous expression of Cbfa1 in nonhypertrophic chondrocytes uncovers its ability to induce hypertrophic chondrocyte differentiation and partially rescues Cbfa1-deficient mice. Genes Dev. 2001;15(4):467–81.

192. Ueta C, Iwamoto M, Kanatani N, Yoshida C, Liu Y, Enomoto-Iwamoto M, et al. Skeletal malformations caused by overexpression of Cbfa1 or its dominant negative form in chondrocytes. J Cell Biol. 2001;153(1):87–100.

193. D'Souza RN, Åberg T, Gaikwad J, Cavender A, Owen M, Karsenty G, et al. Cbfa1 is required for epithelial-mesenchymal interactions regulating tooth development in mice. Development. 1999;126(13):2911–20.

194. Yoshida CA, Yamamoto H, Fujita T, Furuichi T, Ito K, Inoue K ichi, et al. Runx2 and Runx3 are essential for chondrocyte maturation, and Runx2 regulates limb growth through induction of Indian hedgehog. Genes Dev. 2004;18(8):952–63.

195. Pratap J, Lian JB, Javed A, Barnes GL, Van Wijnen AJ, Stein JL, et al. Regulatory roles of Runx2 in metastatic tumor and cancer cell interactions with bone. Cancer and Metastasis Reviews. 2006;25:589–600.

196. Kozhemyakina E, Lassar AB, Zelzer E. A pathway to bone: signaling molecules and transcription factors involved in chondrocyte development and maturation. Development. 2015;142(5):817–31.

197. Symon A, Harley V. SOX9: A genomic view of tissue specific expression and action. Int J Biochem Cell Biol. 2017;87:18–22.

198. Lefebvre V, Dvir-Ginzberg M. SOX9 and the many facets of its regulation in the chondrocyte lineage. Connect Tissue Res. 2017;58(1):2–14.

199. Nishimura R, Hata K, Nakamura E, Murakami T, Takahata Y. Transcriptional network systems in cartilage development and disease. Histochem Cell Biol. 2018;149:353–63.

200. Kawakami Y, Tsuda M, Takahashi S, Taniguchi N, Esteban CR, Zemmyo M, et al. Transcriptional coactivator PGC-1α regulates chondrogenesis via association with Sox9. Proceedings of the National Academy of Sciences. 2005;102(7):2414–9.

201. Hattori T, Müller C, Gebhard S, Bauer E, Pausch F, Schlund B, et al. SOX9 is a major negative regulator of cartilage vascularization, bone marrow formation and endochondral ossification. Development. 2010;137(6):901–11.

202. Ito T, Yadav N, Lee J, Furumatsu T, Yamashita S, Yoshida K, et al. Arginine methyltransferase CARM1/PRMT4 regulates endochondral ossification. BMC Dev Biol. 2009;9:1–10.

203. Tyson KL, Reynolds JL, McNair R, Zhang Q, Weissberg PL, Shanahan CM. Osteo/chondrocytic transcription factors and their target genes exhibit distinct patterns of expression in human arterial calcification. Arterioscler Thromb Vasc Biol. 2003;23(3):489–94.

204. Neven E, Dauwe S, De Broe ME, D'haese PC, Persy V. Endochondral bone formation is involved in media calcification in rats and in men. Kidney Int. 2007;72(5):574–81.

205. Xu Z, Ji G, Shen J, Wang X, Zhou J, Li L. SOX9 and myocardin counteract each other in regulating vascular smooth muscle cell differentiation. Biochem Biophys Res Commun. 2012;422(2):285–90.

206. Jiawen S, Jianjun Z, Jiewen D, Dedong Y, Hongbo Y, Jun S, et al. Osteogenic Differentiation of Human Amniotic Epithelial Cells and Its Application in Alveolar Defect Restoration. Stem Cells Transl Med [Internet]. 2014 Dec 1;3(12):1504–13. Available from: https://doi.org/10.5966/sctm.2014-0118

207. Jia Z, Wang S, He D, Cui L, Lu Y, Hu H, et al. Role of calcium in the regulation of bone morphogenetic protein 2, runt-related transcription factor 2 and Osterix in primary renal tubular epithelial cells by the vitamin D receptor. Mol Med Rep. 2015;12(2):2082–8.

208. Someya H, Fujiwara H, Nagata K, Wada H, Hasegawa K, Mikami Y, et al. Thymosin beta 4 is associated with RUNX2 expression through the Smad and Akt signaling pathways in mouse dental epithelial cells. Int J Mol Med. 2015;35(5):1169–78.

209. Ferrari N, Riggio AI, Mason S, McDonald L, King A, Higgins T, et al. Runx2 contributes to the regenerative potential of the mammary epithelium. Sci Rep. 2015;5(1):15658.

210. Kumar S, Liu J, Pang P, Krautzberger AM, Reginensi A, Akiyama H, et al. Sox9 activation highlights a cellular pathway of renal repair in the acutely injured mammalian kidney. Cell Rep. 2015;12(8):1325–38.

211. Lee YS, Kim J whan, Osborne O, Sasik R, Schenk S, Chen A, et al. Increased adipocyte O2 consumption triggers HIF-1α, causing inflammation and insulin resistance in obesity. Cell. 2014;157(6):1339–52.

212. Persson P, Palm F. Hypoxia-inducible factor activation in diabetic kidney disease. Curr Opin Nephrol Hypertens. 2017;26(5):345–50.

213. Marfella R, Esposito K, Nappo F, Siniscalchi M, Sasso FC, Portoghese M, et al. Expression of angiogenic factors during acute coronary syndromes in human type 2 diabetes. Diabetes. 2004;53(9):2383–91.

214. B Arden G, Sivaprasad S. Hypoxia and oxidative stress in the causation of diabetic retinopathy. Curr Diabetes Rev. 2011;7(5):291–304.

215. Botusan IR, Sunkari VG, Savu O, Catrina AI, Grünler J, Lindberg S, et al. Stabilization of HIF-1α is critical to improve wound healing in diabetic mice. Proceedings of the National Academy of Sciences. 2008;105(49):19426–31.

216. Fialho M da LS, Abd Jamil AH, Stannard GA, Heather LC. Hypoxia-inducible factor 1 signalling, metabolism and its therapeutic potential in cardiovascular disease. Biochimica et Biophysica Acta (BBA)-Molecular Basis of Disease. 2019;1865(4):831–43.

217. Gu HF, Zheng X, Abu Seman N, Gu T, Botusan IR, Sunkari VG, et al. Impact of the hypoxia-inducible factor-1 α (HIF1A) Pro582Ser polymorphism on diabetes nephropathy. Diabetes Care. 2013;36(2):415–21.

218. Catrina SB, Okamoto K, Pereira T, Brismar K, Poellinger L. Hyperglycemia regulates hypoxia-inducible factor-1α protein stability and function. Diabetes. 2004;53(12):3226–32.

219. Takashima M, Nagaya M, Takamura Y, Inatani M, Oki M. HIF-1 inhibition reverses opacity in a rat model of galactose-induced cataract. PLoS One. 2024;19(2):e0299145.

220. Brennan L, Disatham J, Kantorow M. Hypoxia regulates the degradation of non-nuclear organelles during lens differentiation through activation of HIF1a. Exp Eye Res. 2020;198:108129.

221. Rathore R, Zheng YM, Niu CF, Liu QH, Korde A, Ho YS, et al. Hypoxia activates NADPH oxidase to increase [ROS] i and [Ca2+] i through the mitochondrial ROS-PKCε signaling axis in pulmonary artery smooth muscle cells. Free Radic Biol Med. 2008;45(9):1223–31.

222. Nangaku M, Eckardt KU. Hypoxia and the HIF system in kidney disease. J Mol Med. 2007;85:1325–30.

223. Gunaratnam L, Bonventre J V. HIF in kidney disease and development. Journal of the American Society of Nephrology. 2009;20(9):1877–87.

224. Babitt JL, Lin HY. Mechanisms of anemia in CKD. Journal of the American Society of Nephrology. 2012;23(10):1631–4.

225. Norman JT, Clark IM, Garcia PL. Hypoxia promotes fibrogenesis in human renal fibroblasts. Kidney Int. 2000;58(6):2351–66.

226. Manotham K, Tanaka T, Matsumoto M, Ohse T, Inagi R, Miyata T, et al. Transdifferentiation of cultured tubular cells induced by hypoxia. Kidney Int. 2004;65(3):871–80.

227. Querfeld U, Mak RH, Pries AR. Microvascular disease in chronic kidney disease: the base of the iceberg in cardiovascular comorbidity. Clin Sci. 2020;134(12):1333–56.

228. Tani T, Orimo H, Shimizu A, Tsuruoka S. Development of a novel chronic kidney disease mouse model to evaluate the progression of hyperphosphatemia and associated mineral bone disease. Sci Rep. 2017;7(1):2233.

229. Jia T, Olauson H, Lindberg K, Amin R, Edvardsson K, Lindholm B, et al. A novel model of adenine-induced tubulointerstitial nephropathy in mice. BMC Nephrol. 2013;14:1–8.

230. Tanaka T, Doi K, Maeda-Mamiya R, Negishi K, Portilla D, Sugaya T, et al. Urinary L-type fatty acid-binding protein can reflect renal tubulointerstitial injury. Am J Pathol. 2009;174(4):1203–11.

231. Santana AC, Degaspari S, Catanozi S, Dellê H, de Sá Lima L, Silva C, et al. Thalidomide suppresses inflammation in adenine-induced CKD with uraemia in mice. Nephrology dialysis transplantation. 2013;28(5):1140–9.

232. Greco A, Herrmann J, Babic M, Gummi MR, van der Giet M, Tölle M, et al. Molecular imaging and quantification of smooth muscle cell and aortic tissue calcification in vitro and ex vivo with a fluorescent hydroxyapatite-specific probe. Biomedicines. 2022;10(9):2271.

233. Bonewald LF, Harris SE, Rosser J, Dallas MR, Dallas SL, Camacho NP, et al. von Kossa staining alone is not sufficient to confirm that mineralization in vitro represents bone formation. Calcif Tissue Int. 2003;72:537–47.

234. Rungby J, Kassem M, Eriksen EF, Danscher G. The von Kossa reaction for calcium deposits: silver lactate staining increases sensitivity and reduces background. Histochem J. 1993;25:446–51.

235. Herrmann J, Gummi MR, Xia M, van der Giet M, Tölle M, Schuchardt M. Vascular Calcification in Rodent Models—Keeping Track with an Extented Method Assortment. Biology (Basel). 2021;10(6):459.

236. Smith ER, Hewitson TD, Cai MMX, Aghagolzadeh P, Bachtler M, Pasch A, et al. A novel fluorescent probe-based flow cytometric assay for mineral-containing nanoparticles in serum. Sci Rep. 2017;7(1):5686.

237. Charest A, Pepin A, Shetty R, Côté C, Voisine P, Dagenais F, et al. Distribution of SPARC during neovascularisation of degenerative aortic stenosis. Heart. 2006;92(12):1844–9.

238. Katsi V, Magkas N, Antonopoulos A, Trantalis G, Toutouzas K, Tousoulis D. Aortic valve: Anatomy and structure and the role of vasculature in the degenerative process. Acta Cardiol. 2021;76(4):335–48.

239. Soini Y, Salo T, Satta J. Angiogenesis is involved in the pathogenesis of nonrheumatic aortic valve stenosis. Hum Pathol. 2003;34(8):756–63.

240. Perrotta I, Moraca FM, Sciangula A, Aquila S, Mazzulla S. HIF-1α and VEGF: immunohistochemical profile and possible function in human aortic valve stenosis. Ultrastruct Pathol. 2015;39(3):198–206.

241. Fu B, Wang J, Wang L, Wang Q, Guo Z, Xu M, et al. Integrated proteomic and metabolomic profile analyses of cardiac valves revealed molecular mechanisms and targets in calcific aortic valve disease. Front Cardiovasc Med. 2022;9:944521.

242. Parra-Izquierdo I, Castaños-Mollor I, López J, Gómez C, San Román JA, Crespo MS, et al. Lipopolysaccharide and interferon-γ team up to activate HIF-1α via STAT1 in normoxia and exhibit sex differences in human aortic valve interstitial cells. Biochimica et Biophysica Acta (BBA)-Molecular Basis of Disease. 2019;1865(9):2168–79.

243. Mu Y, Gao W, Zhou Y, Xiao L, Xiao Y. Physiological and pathological/ectopic mineralization: from composition to microstructure. Vol. 3, Microstructures. OAE Publishing Inc.; 2023.

244. Li T, Yu H, Zhang D, Feng T, Miao M, Li J, et al. Matrix Vesicles as a Therapeutic Target for Vascular Calcification. Vol. 10, Frontiers in Cell and Developmental Biology. Frontiers Media S.A.; 2022.

245. Ikeda H, Kakeya H. Targeting hypoxia-inducible factor 1 (HIF-1) signaling with natural products toward cancer chemotherapy. Vol. 74, Journal of Antibiotics. Springer Nature; 2021. p. 687–95.

11. Appendix

UNIVERSITY AND NATIONAL LIBRARY
UNIVERSITY OF DEBRECEN
H-4002 Egyetem tér 1, Debrecen
Phone: +3652/410-443, email: publikaciok@lib.unideb.hu

Registry number: DEENK//2024.PL
Subject: PhD Publication List

Candidate: Haneen Muntasir Ababneh
Doctoral School: Doctoral School of Molecular Cellular and Immune Biology

List of publications related to the dissertation

1. **Ababneh, H. M.**, Balogh, E., Csiki, D. M., Lente, G., Fenyvesi, F., Tóth, A., Jeney, V.: High glucose promotes osteogenic differentiation of human lens epithelial cells through hypoxia-inducible factor (HIF) activation.
   J. Cell. Physiol. [Epub ahead of print], 2024.
   DOI: http://dx.doi.org/10.1002/jcp.31211
   IF: 5.6 (2022)

2. Csiki, D. M.*, **Ababneh, H. M.***, Tóth, A., Lente, G., Szöőr, Á., Tóth, A., Fillér, C., Juhász, T., Nagy, B. J., Balogh, E., Jeney, V.: Hypoxia-inducible factor activation promotes osteogenic transition of valve interstitial cells and accelerates aortic valve calcification in a mice model of chronic kidney disease.
   Front. Cardiovasc. Med. 10, 1-15, 2023.
   DOI: http://dx.doi.org/10.3389/fcvm.2023.1168339
   * These authors contributed equally to this work.
   IF: 3.6 (2022)

3. Chowdhury, A., Balogh, E., **Ababneh, H. M.**, Tóth, A., Jeney, V.: Activation of Nrf2/HO-1 Antioxidant Pathway by Heme Attenuates Calcification of Human Lens Epithelial Cells.
   Pharmaceuticals (Basel). 15 (5), 1-13, 2022.
   DOI: http://dx.doi.org/10.3390/ph15050493
   IF: 4.6

UNIVERSITY AND NATIONAL LIBRARY
UNIVERSITY OF DEBRECEN
H-4002 Egyetem tér 1, Debrecen
Phone: +3652/410-443, email: publikaciok@lib.unideb.hu

List of other publications

4. Tóth, A., Csiki, D. M., Nagy, B. J., Balogh, E., Lente, G., **Ababneh, H. M.**, Szöőr, Á., Jeney, V.: Daprodustat Accelerates High Phosphate-Induced Calcification Through the Activation of HIF-1 Signaling.
   Front. Pharmacol. 13, 1-12, 2022.
   DOI: http://dx.doi.org/10.3389/fphar.2022.798053
   IF: 5.6

5. Balogh, E., Chowdhury, A., **Ababneh, H. M.**, Csiki, D. M., Tóth, A., Jeney, V.: Heme-Mediated Activation of the Nrf2/HO-1 Axis Attenuates Calcification of Valve Interstitial Cells.
   Biomedicines. 9 (4), 1-17, 2021.
   DOI: http://dx.doi.org/10.3390/biomedicines9040427
   IF: 4.757

Total IF of journals (all publications): 24,157
Total IF of journals (publications related to the dissertation): 13,8

The Candidate's publication data submitted to the iDEa Tudóstér have been validated by DEENK on the basis of the Journal Citation Report (Impact Factor) database.

25 March, 2024